

Research Article

Robust Distribution-Free Hybrid Exponentially Weighted Moving Average Schemes Based on Simple Random Sampling and Ranked Set Sampling Techniques

Jean-Claude Malela-Majika ¹, Sandile C. Shongwe ², Muhammad Aslam ³,
and Saddam A. Abbasi ⁴

¹Department of Statistics, Faculty of Natural and Agricultural Sciences, University of Pretoria, Hatfield 0002, South Africa

²Department of Mathematical Statistics and Actuarial Science, Faculty of Natural and Agricultural Sciences, University of the Free State, Bloemfontein 9301, South Africa

³Department of Statistics, Faculty of Science, King Abdulaziz University, Jeddah 21551, Saudi Arabia

⁴Department of Mathematics, Statistics & Physics, Qatar University, Doha, Qatar

Correspondence should be addressed to Sandile C. Shongwe; shongwesc@ufs.ac.za

Received 14 May 2021; Accepted 6 July 2021; Published 27 July 2021

Academic Editor: Amer Al-Omari

Copyright © 2021 Jean-Claude Malela-Majika et al. This is an open access article distributed under the Creative Commons Attribution License, which permits unrestricted use, distribution, and reproduction in any medium, provided the original work is properly cited.

This paper proposes new nonparametric hybrid exponentially weighted moving average (HEWMA) control charts based on simple random sampling (SRS) and ranked set sampling (RSS) techniques using the Wilcoxon rank-sum (W) statistic. The in-control robustness and out-of-control (OOC) performances are thoroughly investigated using extensive simulations. The HEWMA W chart is shown to be superior to the basic exponentially weighted moving average (EWMA) and double EWMA W charts in many cases under normal and nonnormal distributions. Moreover, the OOC sensitivities of the new HEWMA W -type control charts are further improved by using supplementary 2-of-2 and 2-of-3 standard and improved runs-rules approaches. It is found that the proposed HEWMA W -type charts with runs-rules perform better than the basic HEWMA W SRS and RSS charts. Real-life data based on the impurity of iron ore are used to illustrate the design and implementation of the new control charts.

1. Introduction

Control charts (also known as monitoring schemes) are statistical tools that help to efficiently monitor a wide range of industrial and nonindustrial processes. These tools are expected to give an out-of-control (OOC) signal as soon as possible when there is a significant change (or shift) in the process parameters or the distribution of the quality characteristic from an in-control (IC) state. Control charts are classified into two main classes, namely, the memoryless (such as the Shewhart chart) and memory-type (such as the exponentially weighted moving average (EWMA) and cumulative sum (CUSUM) charts); see, for example, the study of Montgomery [1], Qiu [2], and Chakraborti and Graham [3]. The Shewhart-type control charts are the oldest and

most popular monitoring schemes. These tools are preferred because of their simplicity and high speed in detecting large shifts in the process parameters. Note though that they are relatively slow in detecting small-to-moderate shifts in the process parameters. To overcome this problem, the statistical process monitoring (SPM) literature recommends the use of the memory-type (i.e., CUSUM and EWMA) control charts. The latter schemes are fast in detecting small-to-moderate shifts and slow in monitoring large shifts. For more details on the enhancement of memory-type schemes, readers are referred to the study carried out by Haq [4], Haq [5], Khoo et al. [6], Adeoti [7], Alevizakos et al. [8], Alevizakos et al. [9], and the references therein. For other alternative approaches of control charts, such as the parametric and nonparametric Kullback–Leibler divergence, see, for

instance, the study carried out by Bakdi and Kouadri [10], Bakdi et al. [11], and Bounoua et al. [12].

In general, the challenge in SPM is to design a control chart which is able to efficiently monitor all ranges of shifts (i.e., small, moderate, and large shifts). Shamma and Shamma [13] introduced the double EWMA (DEWMA) \bar{X} chart in order to improve the performance of the EWMA \bar{X} chart in detecting small shifts in the process mean. The DEWMA-type chart is designed by applying the EWMA statistic twice using the same smoothing parameter (denoted as η , with $0 < \eta \leq 1$). In other words, the DEWMA chart is the mixture of two EWMA charts using the same value of η . Zhang and Cheng [14] and Alevizakos et al. [8] also showed that the basic and modified DEWMA charts perform better than the corresponding EWMA charts in detecting small mean shifts. Moreover, they also reported that the performances of the EWMA and DEWMA charts are almost similar in monitoring large shifts in the process parameters. When different values of η (say, η_1 and η_2) are used, the DEWMA chart is termed hybrid EWMA (HEWMA); see Haq [4]. Other authors (see, for instance, [15–17]) have also reported on the performance of the HEWMA chart as being superior to the EWMA chart in detecting small and moderate process mean shifts. More recently, another hybrid-type scheme based on the homogeneously weighted moving average (HWMA) charting statistics was discussed by Adeoti and Koleoso [18], Malela-Majika et al. [19], and Alevizakos et al. [8].

The aforementioned control charts are based on one sample plotting statistics (or point) plotted against the upper control limit (UCL) and lower control limit (LCL). They give an OOC signal when, at any sampling time, a point plots beyond the control limits; otherwise, the process is considered to be IC. This rule is known as the 1-of-1 rule, and a control chart based on such rule is called a basic control chart. In the last three decades, many authors developed various rules in order to improve the performance of the existing control charts. These rules are known as runs-rules (or stopping rules). For more details on the different types of runs-rules, readers are referred to Klein [20], Khoo and Ariffin [21], Antzoulakos and Rakitzis [22], and Shongwe [23] as well as Adeoti and Malela-Majika [24]. In this paper, the standard runs-rules (SRR) and the improved runs-rules (IRR) approaches are considered. In short, the 2-of-2 SRR approach gives an OOC signal when two successive points plot above (below) the UCL (LCL), respectively. However, the IRR approach has the upper and lower warning limits (denoted as UWL and LWL) in addition to the UCL and LCL such that $LCL < LWL < UWL < UCL$. Thus, the 2-of-2 IRR approach gives an OOC signal when either a single point plots beyond the LCL/UCL, or two successive points plot either between the UCL and UWL or between the LCL and LWL.

Many authors have suggested improving memory-type charts by using supplementary runs-rules. For instance, Sheu and Lin [25] and Riaz et al. [26] proposed the use of runs-rules to improve the performance of the generally weighted moving average (GWMA) and CUSUM charts, respectively. Abbas et al. [27] used the 2-of-2 SRR approach

to improve the basic EWMA chart in detecting sudden small shifts in the process mean parameter and used simulations to investigate the performance of the proposed chart. Marvelakis et al. [28] introduced an exact method based on integral equations to investigate the performance of the EWMA chart with runs-rules. Khoo et al. [6] presented a Markov chain approach for evaluating the performance of the EWMA chart with runs-rules to monitor the process location and showed that their performances are not as good as reported in Abbas et al. [27]. Note though that Khoo et al. [6] did not consider the use of the IRR approach, which actually increases considerably the ability to detect large shifts. Despite Khoo et al. [6] warning about the performance of the memory-type charts, we believe that the use of runs-rules applied to these charts must not yet be discarded since Khoo et al. [6] did not investigate the performance of nonparametric EWMA and other memory-type charts (such as the DEWMA, HEWMA) supplemented with SRR and IRR approaches to check whether the findings remain the same. To this end, Adeoti and Malela-Majika [24] proposed the DEWMA \bar{X} control charts with SRR and IRR approaches and observed that it has very interesting run length properties when supplemented with IRR under the assumption of normality. In this paper, we also consider SRR and IRR applied to the DEWMA chart; however, in a nonparametric scenario.

Nonparametric control charts are typically used when the assumption of normality fails to hold or if there is a doubt about the nature of the underlying process distribution; see Qiu [2] and Chakraborti and Graham [3]. A well-known nonparametric test is based on the Wilcoxon rank-sum (W) statistic [29]. In the SPM context, control charts based on the W statistic have been studied by Li et al. [30], Malela-Majika and Rapoo [31], Mukherjee et al. [32], Chong et al. [33], Mabude et al. [34], Tercero-Gomez et al. [35], Triantafyllou [36], and Letshedi et al. [37]. Most of the latter articles were studied under the assumption of simple random sampling (SRS) technique. Note though that structured sampling strategies like the ranked set sampling (RSS) have been recommended in the SPM literature because they reduce variability and thus improve performance of the corresponding control chart; see, for instance, Haq et al. [38], Awais and Haq [39], and Noor-ul-Amin and Tayyab [40]. The RSS technique has many applications in fields like life sciences, agriculture, and medical and environmental sciences because it provides more structure to the gathered observations and increases the amount of information present in the sample; see Singh and Vishwakarma [41]. For other nonparametric procedures based on ranked set sampling in the context of information theory, survival analysis, reliability, and medicine, the readers are referred to the study carried out by Terpstra and Liudahl [42], Chen et al. [43], Mahdizadeh and Strzalkowska-Kominiak [44], Mahdizadeh [45], and Mahdizadeh [46].

In the nonparametric scenario, Malela-Majika and Rapoo [47] and Malela-Majika [48] investigated the performance of the EWMA and DEWMA W charts using the RSS and SRS techniques, respectively. In this paper, a new

nonparametric HEWMA chart based on W statistic using the SRS and RSS techniques for monitoring the location parameter is proposed. Moreover, the new HEWMA W chart is further enhanced using SRR and IRR w -of- $(w + \nu)$ approaches, with $w = 2$ and $\nu = 0$ and 1 ; henceforth, these are denoted by $SRR_{2\text{-of-}(2+\nu)}$ and $IRR_{2\text{-of-}(2+\nu)}$, respectively.

Section 2 provides the basic design of the nonparametric EWMA, DEWMA, and HEWMA control charts. The design procedures of the $SRR_{2\text{-of-}(2+\nu)}$ and $IRR_{2\text{-of-}(2+\nu)}$ approaches are given in Section 3. Section 4 introduces the design and implementation of the new control charts. Section 5 investigates and discusses the IC robustness and OOC performances as well as the comparison with other existing memory-type W charts. Illustrative examples using real-life data are given in Section 6. Finally, concluding remarks are given in Section 7.

2. Distribution-Free EWMA, DEWMA, and HEWMA W Control Charts

This section presents the theoretical framework adopted for the design of the basic EWMA, DEWMA, and HEWMA control charts based on W statistic using the SRS and RSS techniques.

2.1. SRS and RSS Techniques. The SRS technique is the simplest way to get a sample by randomly selecting n observations (or items) from the target population where every element has the same chance of being selected. However, Ganeslingam and Ganesh [49] stated that since quantification of the variable of interest often requires expensive measurements, in some situations in practice, the observations are usually ranked using a cost-effective measurable covariate and, in that case, the RSS technique is preferred because of its low cost and efficiency. The RSS method consists of drawing a set of n simple random samples, each of size n , from a target population and ordering the observations within each sample with respect to a variable of interest from the smallest to the largest. The sample of interest is obtained by taking the first observation from the first sample of n observations, the second observation from the second sample, the third observation from the third sample, and so forth (see Table 1). The rank set sample is then equivalent to the vector of the main diagonal of an $n \times n$ matrix (i.e., n SRS vectors of size n) with ordered observations. Haq et al. [38] showed that the RSS technique reduces variability in the sample of interest and, consequently, improves the sensitivity of any control chart when compared to the SRS technique.

2.2. Wilcoxon Rank-Sum Statistic for Two-Sample Test Using SRS. Let $X_{\text{SRS}} = \{x_i, i = 1, 2, \dots, m\}$ be a Phase I (or

reference) sample of size m collected from an IC process with an unknown continuous cumulative distribution function (cdf) $F(x)$ and $Y_{\text{SRS}} = \{y_j^q, q = 1, 2, \dots, j = 1, 2, \dots, n\}$, the q^{th} Phase II (or test) sample of size $n_q, n_q = n\nu q$. Let $G^q(y)$ be the cdf of the distribution of the q^{th} test sample and assume $G^q(y) = G(y)\forall q$. The process is IC in Phase II when $G = F$. This means that $G(t) = F(t - \delta), \forall t$, where δ is the shift in the mean parameter. Thus, the process is IC if $\delta = 0$. Wilcoxon [29] introduced the W test based on the sum of ranks of a reference sample X_{SRS} when compared with the test sample Y_{SRS} . When combining these two samples in an ascending order, a new set of sizes $(m + n)$, $X'_{\text{SRS}} = \{x'_1, x'_2, \dots, x'_i, \dots, x'_{m+n-1}, x'_{m+n}\}$, can be formed, where $x'_k = x_i$ if x_i is the k^{th} smallest observation in the combined sample, and $x'_k = y_j$ if y_j is the k^{th} smallest observation in the combined sample; $k \in [1: m + n], i \in [1: m]$ and $j \in [1: n]$. After defining $X''_{\text{SRS}} = \{x'_{(1)}, x'_{(2)}, \dots, x'_{(i)}, \dots, x'_{(m+n-1)}, x'_{(m+n)}\}$, the W statistic is then defined as

$$W_{\text{SRS}} = \sum_{i=1}^{m+n} (i \cdot x'_{(i)}), \quad (1)$$

where $x'_{(i)} = 1$ if x'_i comes from the test sample and $x'_{(i)} = 0$ if x'_i comes from the reference sample.

The expected value and variance of W_{SRS} under the assumption of identical distributions are given by (see [30])

$$E(W_{\text{SRS}}) = \mu_{W_{\text{SRS}}} = \frac{m(m+n+1)}{2}, \quad (2a)$$

and

$$\text{Var}(W_{\text{SRS}}) = \sigma_{W_{\text{SRS}}}^2 = \frac{mn(m+n+1)}{12}, \quad (2b)$$

respectively.

2.3. Wilcoxon Rank-Sum Statistic for Two-Sample Test Using RSS. Let

$Y_{\text{RSS}} = \{y_{(s)j}^h; s = 1, 2, \dots, n; j = 1, 2, \dots, n; h \in N\}$ be a RSS of size n obtained from n independent random samples of size n , each associated with the SRS observations for h cycles with a continuous cdf $G^*(\tau)$. Assume $X_{\text{RSS}} = \{x_{(i)t}^k; i = 1, 2, \dots, m; t = 1, 2, \dots, m; k \in N\}$ is a RSS of size m obtained from m independent samples each associated with the SRS observations for k cycles with a continuous cdf $F^*(\tau)$, with $G^*(\tau) = F^*(\tau - \delta)$, for all τ , where δ is the shift (or change) in the mean (i.e., location) parameter and $-\infty < \delta < \infty$. Under the IC state, $F^* \equiv G^*$. Thus, Bohn and Wolfe [50] showed that under perfect judgement ranking, the RSS pooled sample observations are independent order statistics with a joint probability density function (pdf) defined by (see also [51] and [52])

TABLE 1: The sampling procedure of the RSS technique.

Sets of n unordered observations	Sets of n ordered observations	Final RSS sample
1: $x_{11} \quad x_{21} \quad \dots \quad x_{n1}$	$\mathbf{x}_{(1)1} \quad \mathbf{x}_{(2)1} \quad \dots \quad \mathbf{x}_{(n)1}$	$\{\mathbf{x}_{(1)2}, \mathbf{x}_{(2)2}, \dots, \mathbf{x}_{(n)n}\}$
2: $x_{12} \quad x_{22} \quad \dots \quad x_{n2}$	$\mathbf{x}_{(1)2} \quad \mathbf{x}_{(2)2} \quad \dots \quad \mathbf{x}_{(n)2}$	
$\vdots \quad \vdots \quad \vdots \quad \vdots$	$\vdots \quad \vdots \quad \vdots \quad \vdots$	
$n: \quad x_{1n} \quad x_{2n} \quad \dots \quad x_{mn}$	$\mathbf{x}_{(1)n} \quad \mathbf{x}_{(2)n} \quad \dots \quad \mathbf{x}_{(n)n}$	

$$f_{\text{RSS}}^*(x_{(i)}, y_{(s)}) = \left\{ \prod_{i=1}^m (m-i+1) \binom{m}{i-1} [F^*(x_{(i)})]^{i-1} [1-F^*(x_{(i)})]^{m-1} f^*(x_{(i)}) \right\} \times \left\{ \prod_{s=1}^n \prod_{i=1}^m (n-s+1) \binom{n}{s-1} [[F^*(x_{(s)})]^{s-1} [1-F^*(x_{(s)})]^{n-1} f^*(x_{(s)})] \right\}, \quad (3)$$

where $f^*(\cdot)$ is a continuous pdf of a RSS.

Amro and Samoh [53] showed that the W test statistic using RSS is defined by

$$W_{\text{RSS}} = \sum_{s=1}^m \sum_{t=1}^k R_{st}, \quad (4)$$

where R_{st} is the rank of $Y_{(s)t}$ in the combined sample $\{X_{(i)j}, Y_{(s)t} : i = 1, 2, \dots, m, s = 1, 2, \dots, n\}$ of size $n+m$. Hence,

$$W_{\text{RSS}} = \frac{1}{2} m k (m k + 1) + U_{\text{RSS}}, \quad (5)$$

where the test statistic $U_{\text{RSS}} = \sum_{i=1}^m \sum_{j=1}^h \sum_{s=1}^n \sum_{t=1}^k I(X_{(i)j} < Y_{(s)t})$ is the number of X 's less than or equal to Y 's in the RSS of the combined sample. Thus, the expected value of the two-sample U statistic is defined by

$$E(U_{\text{RSS}}) = \frac{1}{2} m n h k \left(1 + 2 \int_0^\delta \int_{-\infty}^\infty f(y) f(y-x) dy dx \right), \quad (6)$$

where $f(\cdot)$ is a continuous pdf of the SRS technique.

In control, $F^* \equiv G^*$ ($\delta = 0$). Let us assume we have γ cycles for both phases; that is, $h = k = \gamma$. Then,

$$E(U_{\text{RSS}}) = \frac{1}{2} m n \gamma^2. \quad (7)$$

Hence, the expectation of the W statistic is given by

$$E(W_{\text{RSS}}) = \mu_{W_{\text{RSS}}} = \frac{1}{2} m \gamma [(m+n)\gamma + 1]. \quad (8)$$

When $h = k = 1$ (i.e., $\gamma = 1$),

$$\mu_{W_{\text{RSS}}} = \mu_{W_{\text{SRS}}} = \frac{m(m+n+1)}{2}. \quad (9)$$

Note that when $h = k = \gamma \neq 1$, the variance of the two-sample statistic is defined by

$$\text{Var}(W_{\text{RSS}}) = \sigma_{W_{\text{RSS}}}^2 = \text{Var}(W_{\text{SRS}}) - \frac{1}{\gamma m^2} \sum_{t=1}^{\gamma} (\mu_{W_{[t]}} - \mu_{W_{\text{RSS}}})^2, \quad (10)$$

where $\mu_{W_{[t]}}$ is the mean of the W test statistic using RSS at the t^{th} cycle, $\mu_{W_{\text{RSS}}}$ is defined in (8) or (9), and $\text{Var}(W_{\text{SRS}}) = \sigma_{W_{\text{SRS}}}^2 = (mn(m+n+1)/12)$.

2.4. The EWMA W Control Charts. The plotting statistic of the EWMA chart of Li et al. [30] is denoted by W -EWMA. Thus, the W -EWMA statistics based on the W_{SRS} and W_{RSS} statistics at time t are defined by

$$Y_{\text{SRS}_t} = \eta W_{\text{SRS}_t} + (1-\eta) Y_{\text{SRS}_{t-1}}, \quad \text{for } t = 1, 2, 3, \dots, \quad (11a)$$

and

$$Y_{\text{RSS}_t} = \eta W_{\text{RSS}_t} + (1-\eta) Y_{\text{RSS}_{t-1}}, \quad \text{for } t = 1, 2, 3, \dots, \quad (11b)$$

respectively, where $0 < \eta \leq 1$ is a constant known as the smoothing parameter. The initial values Y_{SRS_0} and Y_{RSS_0} are set to be equal to the mean; i.e., $Y_{\text{SRS}_0} = E(W_{\text{SRS}})$ and $Y_{\text{RSS}_0} = E(W_{\text{RSS}})$.

The expected values and exact variances of Y_{SRS_t} and Y_{RSS_t} are given by

$$E(Y_{\text{SRS}_t}) = \mu_{W_{\text{SRS}}}, \quad (12a)$$

$$\text{Var}(Y_{\text{SRS}_t}) = \sigma_{W_{\text{SRS}}}^2 \left(\frac{\eta}{2-\eta} \right) (1 - (1-\eta)^{2t}),$$

and

$$E(Y_{\text{RSS}_t}) = \mu_{W_{\text{RSS}}}, \quad (12b)$$

$$\text{Var}(Y_{\text{RSS}_t}) = \sigma_{W_{\text{RSS}}}^2 \left(\frac{\eta}{2-\eta} \right) (1 - (1-\eta)^{2t}),$$

respectively.

However, when the charts have been running for a very long time, the term $(1 - (1-\eta)^{2t}) \rightarrow 1$; thus, the expected values and asymptotic variances of the proposed W -EWMA SRS and RSS plotting statistics are then defined by

$$E(Y_{SRS_t}) = \mu_{W_{SRS}},$$

$$\text{Var}(Y_{SRS_t}) = \sigma_{W_{SRS}}^2 \left(\frac{\eta}{2 - \eta} \right),$$
(12c)

and

$$E(Y_{RSS_t}) = \mu_{W_{RSS}},$$

$$\text{Var}(Y_{RSS_t}) = \sigma_{W_{RSS}}^2 \left(\frac{\eta}{2 - \eta} \right),$$
(12d)

respectively.

For simplicity, this paper will focus on the asymptotic case (hereafter, Case A). Thus, the asymptotic UCL and LCL of the W-EWMA chart using SRS and RSS are defined by

$$\frac{\text{EUCL}_{SRS}}{\text{ELCL}_{SRS}} = \mu_{W_{SRS}} \pm L_{E_{SRS}} \sigma_{W_{SRS}} \sqrt{\frac{\eta}{2 - \eta}},$$
(12e)

and

$$\frac{\text{EUCL}_{RSS}}{\text{ELCL}_{RSS}} = \mu_{W_{RSS}} \pm L_{E_{RSS}} \sigma_{W_{RSS}} \sqrt{\frac{\eta}{2 - \eta}},$$
(12f)

respectively, where the control limit constants $L_{E_{SRS}}$ and $L_{E_{RSS}}$ are chosen according to design conditions (i.e., choice of η and the nominal ARL_0 value). The basic W-EWMA chart with SRS (RSS) gives a signal if Y_{SRS_t} (Y_{RSS_t}) falls outside of the control limits; that is, Y_{SRS_t} (Y_{RSS_t}) \geq EUCL_{SRS} (EUCL_{RSS}) or Y_{SRS_t} (Y_{RSS_t}) \leq ELCL_{SRS} (ELCL_{RSS}).

2.5. The DEWMA W Control Charts. The DEWMA W control chart (hereafter, W-DEWMA) is a weighted combination of the current and previous information (i.e., observations) by performing exponential smoothing procedure twice. From Malela-Majika [48], the charting statistic of the W-DEWMA control chart using SRS, denoted as Z_{SRS_t} , is defined by

$$Z_{SRS_t} = \eta Y_{SRS_t} + (1 - \eta) Z_{SRS_{t-1}},$$
(13)

where Y_{SRS_t} is defined in (11a) and W_{SRS_t} is defined in (1). The starting values Y_{SRS_0} and Z_{SRS_0} are equal to the $\mu_{W_{SRS}}$ (i.e., $Y_{SRS_0} = Z_{SRS_0} = \mu_{W_{SRS}}$).

It can be shown that (13) can also be written as [54]

$$Z_{SRS_t} = \eta^2 \sum_{j=1}^t (t - j + 1) (1 - \eta)^{t-j} W_{SRS_j} + t\eta (1 - \eta)^t Y_{SRS_0} + (1 - \eta)^t Z_{SRS_0}.$$
(14)

The asymptotic expected value and variance of the W-DEWMA statistic are given as

$$E(Z_{SRS_t}) = \mu_{Z_{SRS}} = \mu_{W_{SRS}}$$
(15a)

and

$$\text{Var}(Z_{SRS_t}) = \sigma_{Z_{SRS}}^2 = \frac{\eta(2 - 2\eta + \eta^2)}{(2 - \eta)^3} \sigma_{W_{SRS}}^2,$$
(15b)

where $\mu_{W_{SRS}}$ and $\sigma_{W_{SRS}}^2$ are defined in Section 2.3.

From (11b), the charting statistic of the W-DEWMA control chart using RSS, denoted Z_{RSS_t} , is defined as follows:

$$Z_{RSS_t} = \eta Y_{RSS_t} + (1 - \eta) Z_{RSS_{t-1}},$$
(16)

where $Y_{RSS_t} = \eta W_{RSS_t} + (1 - \eta) Y_{RSS_{t-1}}$, W_{RSS_t} is the charting statistic of the t^{th} RSS test sample. The starting values Y_{RSS_0} and Z_{RSS_0} are typically taken to be equal to the $\mu_{W_{RSS}}$ (i.e., $Y_{RSS_0} = Z_{RSS_0} = \mu_{W_{RSS}}$) where $\mu_{W_{RSS}}$ is defined in Section 2.3.

The properties of the W-DEWMA chart using RSS can be defined in a similar way to those of the W-DEWMA chart using SRS by replacing the subscript SRS with RSS. The asymptotic UCL and LCL of the W-DEWMA control chart using SRS and RSS are given by

$$\frac{\text{DUCL}_{SRS}}{\text{DLCL}_{SRS}} = \mu_{W_{SRS}} \pm L_{D_{SRS}} \sigma_{W_{SRS}} \sqrt{\frac{\eta(2 - 2\eta + \eta^2)}{(2 - \eta)^3}},$$
(17a)

and

$$\frac{\text{DUCL}_{RSS}}{\text{DLCL}_{RSS}} = \mu_{W_{RSS}} \pm L_{D_{RSS}} \sigma_{W_{RSS}} \sqrt{\frac{\eta(2 - 2\eta + \eta^2)}{(2 - \eta)^3}},$$
(17b)

respectively, where $L_{D_{SRS}}$ and $L_{D_{RSS}}$ are the control limit constants of the W-DEWMA chart and they are chosen according to design conditions (i.e., choice of η and the nominal ARL_0 value).

The W-DEWMA chart gives an OOC signal if the plotting statistic falls outside of the control limits. Henceforth, the W-DEWMA control charts based on the W using SRS and RSS will be denoted as W-DEWMA SRS and W-DEWMA RSS control charts, respectively.

2.6. The Proposed HEWMA W Control Charts. The HEWMA W control chart (hereafter, W-HEWMA) is a weighted combination of the current and previous information by applying the W-EWMA statistic twice using different smoothing parameters. The plotting statistics of the W-HEWMA chart using SRS and RSS, denoted as H_{SRS_t} and H_{RSS_t} , are defined by

$$H_{SRS_t} = \eta_2 Y_{SRS_t} + (1 - \eta_2) H_{SRS_{t-1}}, \quad 0 < \eta_2 \leq 1,$$
(18a)

and

$$H_{RSS_t} = \eta_2 Y_{RSS_t} + (1 - \eta_2) H_{RSS_{t-1}},$$
(18b)

respectively, where $Y_{SRS_t} = \eta_1 W_{SRS_t} + (1 - \eta_1) Y_{SRS_{t-1}}$ and $Y_{RSS_t} = \eta_1 W_{RSS_t} + (1 - \eta_1) Y_{RSS_{t-1}}$ with $0 < \eta_\tau \leq 1$ (with $\tau = 1$ and 2); W_{SRS_t} and W_{RSS_t} are the charting statistics of the t^{th} SRS and RSS test samples, respectively. The starting values H_{SRS_0} and H_{RSS_0} are also taken to be equal to the $\mu_{W_{SRS}}$ and $\mu_{W_{RSS}}$, respectively.

By following a similar approach to that of Haq [4], the asymptotic expected value and variance of the W-HEWMA statistic using SRS are given as

$$E(H_{\text{SRS}}) = \mu_{H_{\text{SRS}}} = \mu_{W_{\text{SRS}}}, \quad (19a)$$

and

$$\text{Var}(H_{\text{SRS}}) = \sigma_{H_{\text{SRS}}}^2 = \frac{\eta_1^2 \eta_2^2}{(\eta_1 - \eta_2)^2} \left\{ \frac{(\eta_1')^2}{1 - (\eta_1')^2} + \frac{(\eta_2')^2}{1 - (\eta_2')^2} - \frac{2\eta_1' \eta_2'}{1 - \eta_1' \eta_2'} \right\} \sigma_{W_{\text{SRS}}}^2, \quad (19b)$$

respectively, where $\eta_1' = 1 - \eta_1$, $\eta_2' = 1 - \eta_2$, with $\mu_{W_{\text{SRS}}}$ and $\sigma_{W_{\text{SRS}}}^2$ defined in Section 2.3. The asymptotic properties of the W-HEWMA chart using RSS technique can also be defined in a similar manner. Thus, the asymptotic UCL and LCL of the W-HEWMA chart using SRS and RSS are defined by

$$\frac{\text{HUCL}_{\text{SRS}}}{\text{HLCL}_{\text{SRS}}} = \mu_{W_{\text{SRS}}} \pm L_{H_{\text{SRS}}} \sigma_{H_{\text{SRS}}}, \quad (20a)$$

and

$$\frac{\text{HUCL}_{\text{RSS}}}{\text{HLCL}_{\text{RSS}}} = \mu_{W_{\text{RSS}}} \pm L_{H_{\text{RSS}}} \sigma_{H_{\text{RSS}}}, \quad (20b)$$

respectively, where $\sigma_{H_{\text{SRS}}}^2 = (\eta_1^2 \eta_2^2 / (\eta_1 - \eta_2)^2) \{ ((\eta_1')^2 / (1 - (\eta_1')^2) + ((\eta_2')^2 / (1 - (\eta_2')^2)) - (2\eta_1' \eta_2' / (1 - \eta_1' \eta_2')) \} \sigma_{W_{\text{SRS}}}^2$. Note that $L_{H_{\text{SRS}}}$ and $L_{H_{\text{RSS}}}$ are the control limit constants of the W-HEWMA chart and they are chosen according to design conditions (i.e., choice of η_1 and η_2 as well as the nominal ARL_0 value). The W-HEWMA chart gives an OOC signal if a plotting statistic falls beyond the control limits in (20a) and (20b). Henceforth, the W-HEWMA control charts using SRS and RSS techniques will be referred to as W-HEWMA SRS and W-HEWMA RSS control charts, respectively.

To improve the newly proposed W-HEWMA charts as well as the W-EWMA and W-DEWMA SRS and RSS control charts, this study proposes the addition of the $\text{SRR}_{2\text{-of-(}2+\nu)}$ and $\text{IRR}_{2\text{-of-(}2+\nu)}$. The design procedure of the enhanced control charts is given in the next section.

3. The Proposed W-HEWMA Chart with Supplementary Runs-Rules

SRR and IRR are usually added to the basic control chart to improve their detection ability of small, moderate, and large shifts in the process. In this paper, the $\text{SRR}_{2\text{-of-(}2+\nu)}$ and $\text{IRR}_{2\text{-of-(}2+\nu)}$ schemes are used to increase the sensitivity of the proposed memory-type control charts. In this section, three rules are given to describe the proposed control charts where the charting statistics H_{SRS_t} and H_{RSS_t} are simply denoted by H_t , Y_{SRS_t} and Y_{RSS_t} by Y_t , and finally Z_{SRS_t} and Z_{RSS_t} by Z_t .

3.1. Rule 1: $\text{RR}_{1\text{-of-}1}$ (or Basic) Scheme. The $\text{RR}_{1\text{-of-}1}$ control scheme gives a signal whenever the plotting statistic falls on or above the UCL_1 or falls on or below the LCL_1 . The subscript indicates the rule number in order to show that the values of the control limits for the three rules are different. Note that the control chart based on the $\text{RR}_{1\text{-of-}1}$ rule corresponds to the traditional (or basic) control chart.

3.2. Rule 2: $\text{SRR}_{2\text{-of-(}2+\nu)}$. Let P_t (with $t = 1, 2, 3, \dots$) represents the plotting statistic of either the W-HWMA, W-EWMA, or W-DEWMA chart and let $(\text{LCL}_2, \text{UCL}_2)$ represent their corresponding rule 2 pair of control limits. For instance, for the W-HWMA chart, $P_t = H_t$ and $(\text{LCL}_2, \text{UCL}_2) = (\text{HLCL}_2, \text{HUCL}_2)$. The $\text{SRR}_{2\text{-of-(}2+\nu)}$ scheme (with $\nu = 0$ and 1) gives an OOC signal when two out of $2 + \nu$ consecutive charting statistics, say, P_t and P_{t+1} , both fall above (below) the UCL_3 (LCL_3), which are separated by at least ν charting statistics that fall below (above) the LCL_2 (UCL_2), respectively. Therefore, the two-sided $\text{SRR}_{2\text{-of-}2}$ scheme gives an OOC signal at time t if

$$\text{Min}_t(P_t, P_{t+1}) \geq \text{UCL}_2 \quad (21)$$

$$\text{or Max}_t(P_t, P_{t+1}) \leq \text{LCL}_2.$$

However, for the two-sided $\text{SRR}_{2\text{-of-}3}$ scheme, the process is OOC at the sampling time t if one of the following conditions holds:

- (i) $\text{Min}_t(P_t, P_{t+1}) \geq \text{UCL}_2$ or $\text{Max}_t(P_t, P_{t+1}) \leq \text{LCL}_2$
- (ii) $\text{Min}_t(P_t, P_{t+2}) \geq \text{UCL}_2$ or $\text{Max}_t(P_t, P_{t+2}) \leq \text{LCL}_2$
- (iii) $\text{Min}_t(P_{t+1}, P_{t+2}) \geq \text{UCL}_2$ or $\text{Max}_t(P_{t+1}, P_{t+2}) \leq \text{LCL}_2$

3.3. Rule 3: $\text{IRR}_{2\text{-of-(}2+\nu)}$. Let $(\text{LWL}_3, \text{UWL}_3)$ and P_t represent rule 3 pair of the warning limits and plotting statistic of either the W-HWMA, W-EWMA, or W-DEWMA chart. For instance, for the W-HWMA chart, $P_t = H_t$ and $(\text{LWL}_3, \text{UWL}_3) = (\text{HLWL}_3, \text{HUWL}_3)$. Thus, the warning limits, LWL_3 and UWL_3 , of the $\text{IRR}_{2\text{-of-(}2+\nu)}$ W-HEWMA, W-EWMA, and W-DEWMA charts are given by

$$\mu_W \pm L_{H_3} \sigma_W \sqrt{\frac{\eta_1^2 \eta_2^2}{(\eta_1 - \eta_2)^2} \left\{ \frac{(\eta_1')^2}{1 - (\eta_1')^2} + \frac{(\eta_2')^2}{1 - (\eta_2')^2} - \frac{2\eta_1' \eta_2'}{1 - \eta_1' \eta_2'} \right\}}, \quad (22a)$$

$$\mu_W \pm L_{E_3} \sigma_W \sqrt{\frac{\eta}{2 - \eta}}, \quad (22b)$$

and

$$\mu_W \pm L_{D_3} \sigma_W \sqrt{\frac{\eta(2 - 2\eta + \eta^2)}{(2 - \eta)^3}}, \quad (22c)$$

respectively, where μ_W and σ_W represent the expected value and standard deviation of the W statistic using either the SRS or RSS, respectively, and L_{H_3} , L_{E_3} , and L_{D_3} represent the distances of the warning limit (WL) from the CL of the W-HEWMA, W-EWMA, and W-DEWMA control charts, respectively. These distances are chosen such that the attained ARL_0 is in the close vicinity of the nominal ARL_0 value.

Therefore, the IRR_{2-of-3} scheme gives an OOC at time t if one of the following conditions is satisfied:

- (i) $P_t < LCL_3$ or $P_t > UCL_3$
- (ii) $\text{Min}_t(P_t, P_{t+1}) \geq UWL_3$ or $\text{Max}_t(P_t, P_{t+1}) \leq LWL_3$
- (iii) $\text{Min}_t(P_t, P_{t+2}) \geq UWL_3$ or $\text{Max}_t(P_t, P_{t+2}) \leq LWL_3$
- (iv) $\text{Min}_t(P_{t+1}, P_{t+2}) \geq UWL_3$ or $\text{Max}_t(P_{t+1}, P_{t+2}) \leq LWL_3$

Here, LCL_3 and UCL_3 are equivalent to the control limits defined in Section 2. Thus, the IRR W-HEWMA chart has a pair of control limit constants, i.e., (L_H, L_{H_3}) .

4. Design Considerations of the Proposed W-HEWMA Control Charts

The following steps show how to design the W-HEWMA SRS and RSS charts when the process parameters are unknown with one cycle for the RSS case:

Step 1. Draw a reference (i.e., Phase I) sample $X = (x_1, x_2, \dots, x_m)$ from a selected distribution using an SRS or RSS.

Step 2. Draw a test (i.e., Phase II) sample $Y = (y_1, y_2, \dots, y_n)$ from the same distribution as the one in Step 1 using SRS or RSS such that, for the IC state, $\delta = 0$ so that the two distributions (i.e., the ones for Phases I and II) are identical. For the OOC state, the two distributions differ only in the location parameters; we say there is a shift in the mean parameter (i.e., $\delta \neq 0$).

Step 3. The W statistic using SRS and RSS is computed by combining the reference and test samples as explained in Section 2.1 (see also (1) and (4)).

Step 4. Compute the expected value and variance of W based on SRS and RSS when the process is deemed to be IC using (12c) and (12d), respectively.

Step 5. (a) To build the W-HEWMA SRS chart, we use the W_{SRS} statistic from (18a). (b) To build the W-HEWMA RSS chart, we use the W_{RSS} statistic from (18b).

Step 6. The control limit constants and the design parameters of the process are selected such that the attained ARL_0 value is the close vicinity of the nominal $ARL_0 = 500$.

(a) The steady state (or asymptotic) control limits and warning limits for the W-HEWMA SRS chart are calculated using (20a) and (22a), respectively. The RR_{I-of-1} , $SRR_{2-of-(2+v)}$, and $IRR_{2-of-(2+v)}$ charts give a signal if rules 1, 2, and 3 are satisfied, respectively.

(b) The asymptotic control limits and warning limits of the W-HEWMA RSS chart are calculated using (20b) and (22a), respectively. The RR_{I-of-1} , $SRR_{2-of-(2+v)}$, and $IRR_{2-of-(2+v)}$ charts give a signal if rules 1, 2, and 3 are satisfied, respectively.

5. Empirical Discussion of the W-HEWMA Chart with and without Runs-Rules

In this section, intensive Monte Carlo simulations with 50000 iterations are used in SAS®9.4/IML11.42 to evaluate the performance of the proposed W-HEWMA control charts in terms of characteristics of the run length (RL) such as the average RL (ARL) and standard deviation of the RL (SDRL) as well as the 5th, 25th, 50th, 75th, and 95th percentiles of the RL (PRL) which are denoted as P_5 , P_{25} , P_{50} , P_{75} , and P_{95} , respectively.

Note that the aforementioned performance measures are used to investigate the sensitivity of a control chart for a specific shift (δ). However, to evaluate the sensitivity of a control chart for a range of shifts (or overall performance), the expected ARL (EARL) and expected SDRL (ESDRL) metrics are often recommended (see [55]). The EARL and ESDRL are mathematically defined by

$$EARL = \frac{1}{\Delta} \sum_{\delta=\delta_{\min}}^{\delta=\delta_{\max}} ARL(\delta) \tag{23a}$$

and

$$ESDRL = \frac{1}{\Delta} \sum_{\delta=\delta_{\min}}^{\delta=\delta_{\max}} SDRL(\delta), \tag{23b}$$

respectively, where $ARL(\delta)$ and $SDRL(\delta)$ represent the ARL and SDRL for a specific shift of δ standard deviation and Δ is the number of increments between δ_{\min} and δ_{\max} . Note that the smaller the EARL or ESDRL value, the better the performance.

5.1. Robustness of the W-HEWMA SRR and RSS Charts.

A control chart is said to be IC robust if the IC characteristics of the RL distribution are approximately the same across different continuous probability distributions, for instance, when the IC ARL remains closer or equal to the nominal ARL across all continuous distributions; see Chakraborti and Graham [3]. In this paper, to investigate the IC robustness of the proposed charts, three continuous distributions are used, namely, the standard normal distribution (denoted as $N(0,1)$), the Student's t distribution with degrees of freedom $\kappa = 5, 15, 30$ (denoted as $t(\kappa)$), and the gamma distribution with shape parameter $\alpha = 1, 15, 30$ and scale parameter $\beta = 1$ (denoted as $G(\alpha, \beta)$). Table 2 displays the IC RL characteristics of the W-HEWMA charts using the SRS and RSS techniques along with the corresponding control limit coefficient values when $(m, n) = (100, 5)$, $\eta_1 \in \{0.05, 0.1, 0.25, 0.5, 0.75\}$, and $\eta_2 \in \{0.1, 0.25, 0.5, 0.75, 0.9\}$ for a nominal ARL_0 value of 500.

TABLE 2: IC robustness of the W-HEWMA SRS and RSS control charts when $(m, n) = (100, 5)$, $\eta_1 \in \{0.05, 0.1, 0.25, 0.5, 0.75\}$ and $\eta_2 \in \{0.1, 0.25, 0.5, 0.75, 0.9\}$ under different continuous distributions for a nominal ARL_0 of 500

η_1	η_2	L_{SRS} or L_{RSS}	ARL			SDRL			$P_5, P_{25}, P_{50}, P_{75}, P_{95}$		
			$N(0,1)$	$t(5)$	$G(1,1)$	$N(0,1)$	$t(5)$	$G(1,1)$	$N(0,1)$	$t(5)$	$G(1,1)$
W-HEWMA SRS	0.10	2.5482	501.2	510.1	500.2	868.4	866.3	852.5	27,68,184,553,2107	28,69,190,571,2108	28,68,185,557,2058
	0.25	2.6802	499.8	502.9	513.1	899.3	857.9	863.8	25,69,187,550,2002	24,68,187,550,2065	25,69,190,569,2071
	0.50	2.7859	503.0	490.1	500.4	882.7	836.6	870.5	24,68,189,564,2021	23,67,184,538,1978	23,66,188,554,2027
	0.75	2.8469	502.5	496.4	489.0	864.2	850.4	815.1	24,69,191,563,2066	24,67,187,554,2052	24,69,181,534,1919
	0.90	2.8824	502.7	505.9	514.6	886.9	898.1	916.9	24,68,186,558,2077	24,66,186,555,2022	22,68,188,595,2128
	0.25	2.7657	499.9	506.0	506.3	808.6	816.2	837.3	21,71,210,576,1930	20,73,213,599,1966	20,71,202,586,2022
	0.50	2.8653	500.9	498.8	494.8	807.4	818.2	879.0	19,70,211,584,1952	19,79,205,576,1944	20,73,213,587,1935
	0.75	2.9303	499.5	500.9	492.6	838.8	817.5	812.8	19,72,204,573,1967	19,72,209,569,1993	19,71,208,574,1868
	0.90	2.9691	501.1	510.8	512.0	798.5	847.3	860.5	19,74,207,587,1979	19,71,215,598,1944	19,74,215,598,2015
	0.50	2.9508	500.1	504.6	504.6	722.3	747.5	763.4	19,86,246,614,1841	18,88,243,621,1867	18,87,244,608,1834
0.25	2.9915	499.9	494.3	510.1	811.1	723.5	769.9	17,87,244,604,1797	18,87,244,596,1807	18,88,250,614,1849	
0.50	3.0029	500.8	500.0	505.2	812.8	755.9	765.6	18,86,241,613,1799	18,89,242,618,1783	18,86,248,605,1816	
0.75	2.9729	499.4	492.0	497.0	724.5	686.6	738.1	19,99,262,610,1757	17,94,259,609,1743	18,96,255,609,1761	
0.90	2.9566	501.2	504.8	507.9	704.9	728.1	734.8	19,98,265,630,1751	18,99,267,621,1751	19,98,264,623,1782	
0.75	2.8737	502.3	497.4	505.0	698.6	680.5	707.3	19,103,270,633,1733	19,106,274,623,1670	18,108,280,631,1706	
W-HEWMA RSS	0.10	1.2722	502.5	498.9	506.0	511.9	490.3	508.2	46,152,338,680,1553	46,153,345,670,1467	45,153,345,685,1514
	0.25	1.3696	501.2	498.6	497.7	504.7	502.8	501.2	44,153,343,679,1537	43,150,336,678,1503	40,148,336,676,2503
	0.50	1.4403	500.9	502.9	491.7	504.1	495.5	501.9	42,149,340,667,1491	40,149,348,689,1511	39,143,332,676,1481
	0.75	1.4787	500.1	495.6	493.0	492.7	507.3	493.9	41,150,349,698,1463	39,148,339,668,1511	39,149,341,667,1493
	0.90	1.5006	500.0	501.1	493.4	511.6	512.0	497.3	38,149,339,679,1523	39,150,339,672,1512	40,148,340,672,1499
	0.25	1.4553	499.4	511.9	497.7	498.8	516.5	503.8	37,146,337,681,1502	36,148,347,701,1556	35,147,341,680,1476
	0.50	1.5313	500.1	496.7	500.6	498.9	496.4	507.6	33,148,348,678,1503	33,145,342,686,1505	33,145,343,685,1541
	0.75	1.5731	500.9	491.9	502.9	497.1	492.6	510.0	34,150,353,687,1480	34,141,337,684,1470	33,143,345,688,1519
	0.90	1.5972	500.7	505.5	507.8	506.3	507.5	506.7	33,143,348,691,1510	33,148,352,695,1515	33,152,352,695,1536
	0.50	1.6274	500.2	502.6	501.8	510.9	514.7	512.1	31,147,342,681,1510	29,145,344,683,1512	29,147,345,681,1497
0.25	1.6671	501.6	499.5	501.5	507.6	505.2	509.6	28,145,348,695,1520	30,143,341,688,1470	28,144,344,685,1525	
0.50	1.6862	501.1	505.8	498.1	508.4	505.8	506.3	28,140,343,695,1504	31,150,348,693,1519	29,143,346,681,1503	
0.75	1.7132	499.9	505.6	503.7	505.9	507.9	511.3	27,145,342,682,1520	27,142,347,693,1535	28,143,346,689,1526	
0.90	1.7185	499.7	496.6	498.9	509.4	494.2	500.3	26,145,343,683,1498	26,143,342,684,1488	28,146,343,688,1472	
0.75	1.7271	499.6	504.5	500.5	504.9	501.1	499.4	27,144,347,689,1506	28,149,354,697,1525	27,141,348,696,1498	

From Table 2, it can be seen that when η_1 , η_2 , and L (i.e., $L_{H_{SRS}}$ and $L_{H_{RSS}}$) are kept fixed, the variation in the IC characteristics of the RL distribution of the basic W-HEWMA chart using the SRS and RSS techniques is not significant across various probability distributions considered in this paper. For instance, when $(m, n) = (100, 5)$, then for the SRS with $\eta_1 = 0.5$, $\eta_2 = 0.75$, and $L_{H_{SRS}} = 2.9729$, the W-HEWMA chart yields attained IC ARL values of 499.4, 492.0, and 497.0 under the $N(0,1)$, $t(5)$, and $G(1,1)$ distributions, respectively. Moreover, other IC characteristics of the RL distribution are also closer to each other; for instance, the attained P_{50} (also known as the median RL) values are given by 262, 259, and 255 under the $N(0,1)$, $t(5)$, and $G(1,1)$ distributions, respectively. It is important to note that the variability in the IC RL distribution of the W-HEWMA chart using SRS technique is larger compared to the one of the RSS technique; see the IC SDRL values. Finally, the control limit coefficients (i.e., $L_{H_{SRS}}$) of the W-HEWMA charts for the SRS technique are larger compared to those of the RSS technique, which implies that the control limits of the W-HEWMA SRS chart are wider than the ones of the W-HEWMA RSS chart.

The patterns of the IC RL characteristics of the $SRR_{2-of-(2+v)}$ and $IRR_{2-of-(2+v)}$ are similar to the ones in Table 2; for brevity, they are not shown here. Thus, it can be concluded that the W-HEWMA SRS and RSS with and without runs-rules are IC robust.

5.2. OOC Performance of the W-HEWMA SRS and RSS Charts.

In Table 3, four important deductions can be observed. Firstly, it can be observed that, for small η_1 values, both the W-HEWMA SRS and RSS schemes perform worst for small η_2 values. Secondly, the ARL and EARL of the RSS technique are much smaller than those of the SRS technique. To illustrate the latter two deductions empirically, consider Table 3 under the $N(0, 1)$ distribution, with η_1 small (i.e., $\eta_1 = 0.05$): when $\eta_2 = 0.1, 0.25, 0.5, 0.75$, and 0.9 , the W-HEWMA SRS chart yields EARL values (using (23a) and the ARL values shown in Table 3, with $\delta_{\min} = 0.25$ and $\delta_{\max} = 2$) of 19.5, 17.9, 16.9, 15.8, and 16.0, respectively. These show that when η_2 is small, the corresponding ARL values at different shift values are generally higher than those when η_2 is higher. Next, since the W-HEWMA RSS chart yields EARL values of 8.1, 6.2, 5.3, 4.7, and 4.6, respectively, these show that the EARLs of the SRS are higher than those of corresponding RSS technique. A similar pattern is observed under the $t(5)$ and $G(1,1)$ distributions. Thirdly, it can be observed from Table 3 that the W-HEWMA charts perform better under skewed and heavy-tailed distributions, as compared to the normal distribution. It is worth mentioning that the sensitivity of the W-HEWMA chart with smoothing parameters (η_1, η_2) is equivalent to the one of (η_2, η_1) ; that is, when the smoothing parameters are reversed, the performance is the same. Finally, the OOC SDRL values of the W-HEWMA RSS chart are significantly smaller than those of the corresponding W-HEWMA SRS chart.

Figures 1(a) and 1(b) compare the OOC performances of the basic W-HEWMA SRS and RSS charts, respectively, when $(m, n) = (100, 5)$, and $\eta_1 \in \{0.05, 0.5, 0.9\}$ with η_2 fixed

at 0.75 under the $N(0,1)$ distribution. Moreover, the corresponding results of the W-HEWMA SRS and RSS charts under the $t(5)$ distribution are displayed in Figures 1(c) and 1(d), respectively. From Figure 1, it can be seen that regardless of the nature of the underlying distribution, with η_2 fixed to a large value, for small shifts in the process parameters, the W-HEWMA SRS chart performs better with small η_1 values; on the other hand, for large shifts, it performs better with large η_1 values. Note though that the corresponding W-HEWMA RSS chart with small η_1 values performs better for small shifts, while the one with moderate η_1 values performs better for moderate shifts, and for large shifts, it performs similarly for moderate and large values of η_1 . Note that the sensitivity of the W-HEWMA SRS and RSS charts for large shifts is higher when both η_1 and η_2 are large. The pattern of the ARL profile of the W-HEWMA SRS and RSS charts under the $G(1,1)$ using the above scenario is similar to the ones displayed in Figures 1(c) and 1(d); hence, for brevity, they are not shown here.

5.3. The W-HEWMA Chart versus $SRR_{2-of-(2+v)}$ W-HEWMA Chart.

Figure 2 shows OOC performance comparison between the W-HEWMA scheme (without runs-rules) with the ones with the $SRR_{2-of-(2+v)}$ when $v \in \{0, 1\}$ and $(\eta_1, \eta_2) = (0.25, 0.75)$ under the $N(0,1)$ and $t(5)$ distributions. It can be seen that, for small shifts, the W-HEWMA charts are less sensitive than the $SRR_{2-of-(2+v)}$ W-HEWMA charts regardless of the type of the sampling technique. However, for moderate-to-large shifts, the W-HEWMA chart without runs-rules has better performance.

5.4. The W-HEWMA Chart versus $IRR_{2-of-(2+v)}$ W-HEWMA Charts.

Figure 3 compares the OOC performances of the W-HEWMA chart with the ones of the $IRR_{2-of-(2+v)}$ W-HEWMA charts when $v \in \{0, 1\}$ and $(\eta_1, \eta_2) = (0.25, 0.75)$ under the $N(0,1)$ and $t(5)$ distributions. It is observed that, for small shifts in the process location, the $IRR_{2-of-(2+v)}$ W-HEWMA SRS and RSS charts perform better than the W-HEWMA SRS and RSS charts, respectively. However, for large shifts, the W-HEWMA SRS chart outperforms the $IRR_{2-of-(2+v)}$ W-HEWMA SRS chart, while the performances of the W-HEWMA and $IRR_{2-of-(2+v)}$ W-HEWMA charts using the RSS technique are almost similar regardless of the nature of the underlying distribution.

5.5. The $SRR_{2-of-(2+v)}$ W-HEWMA Charts versus $IRR_{2-of-(2+v)}$ W-HEWMA Charts.

Figure 4 compares the OOC performances of the $SRR_{2-of-(2+v)}$ W-HEWMA schemes with the ones of the $IRR_{2-of-(2+v)}$ W-HEWMA schemes when $v \in \{0, 1\}$ and $(\eta_1, \eta_2) = (0.5, 0.9)$ under the $N(0,1)$ and $t(5)$ distributions. For small-to-moderate shifts, the sensitivities of the $SRR_{2-of-(2+v)}$ and $IRR_{2-of-(2+v)}$ W-HEWMA SRS charts are almost similar regardless of the nature of the process underlying distribution, whereas, for large shifts, the $IRR_{2-of-(2+v)}$ W-HEWMA SRS chart is more sensitive than the $SRR_{2-of-(2+v)}$ W-HEWMA SRS chart. However, for small shifts in

TABLE 3: OOC ARL and SDRL profiles of the basic W-HEWMA chart using the SRS (and RSS in parentheses) when $\eta_1 = 0.05$, $\eta_2 \in \{0.1, 0.25, 0.5, 0.75, 0.9\}$, and $(m, n) = (100, 5)$ for a nominal $ARL_0 = 500$

Shift	$\eta_2 = 0.1$			$\eta_2 = 0.25$			$\eta_2 = 0.5$			$\eta_2 = 0.75$			$\eta_2 = 0.9$			
	$N(0,1)$	$t(5)$	$G(1,1)$	$N(0,1)$	$t(5)$	$G(1,1)$	$N(0,1)$	$t(5)$	$G(1,1)$	$N(0,1)$	$t(5)$	$G(1,1)$	$N(0,1)$	$t(5)$	$G(1,1)$	
ARL	0.25	72.8	51.6	31.7	76.5	54.1	29.5	76.1	51.2	26.2	71.3	50.1	33.2	73.5	51.6	32.1
		(16.7)	(15.0)	(11.6)	(14.0)	(12.3)	(9.0)	(13.2)	(11.3)	(7.9)	(12.8)	(10.9)	(7.5)	(12.9)	(11.0)	(7.4)
	0.5	17.5	15.6	12.8	14.6	12.7	10.0	13.7	11.6	8.7	13.3	11.2	8.4	13.3	11.1	8.3
		(10.0)	(9.3)	(7.9)	(7.6)	(7.0)	(5.9)	(6.4)	(5.8)	(4.7)	(6.0)	(5.3)	(4.2)	(5.9)	(5.2)	(4.1)
	0.75	12.5	11.6	10.3	9.7	8.8	7.7	8.5	7.6	6.5	8.1	7.2	6.0	8.0	7.1	5.9
		(7.8)	(7.3)	(6.3)	(5.8)	(5.4)	(4.9)	(4.6)	(4.3)	(3.9)	(4.2)	(3.8)	(3.2)	(4.0)	(3.7)	(3.1)
	1	10.4	9.8	9.1	7.8	7.3	6.7	6.5	6.0	5.5	6.1	5.6	5.0	6.0	5.5	4.9
		(6.7)	(6.3)	(6.0)	(4.9)	(4.6)	(4.0)	(3.8)	(3.6)	(3.1)	(3.3)	(3.1)	(3.0)	(3.2)	(3.0)	(2.9)
1.5	8.5	8.2	8.0	6.2	6.0	5.9	5.0	4.7	4.6	4.5	4.3	4.1	4.3	4.1	4.0	
	(5.6)	(5.3)	(5.0)	(4.0)	(4.0)	(4.0)	(3.0)	(3.0)	(3.0)	(2.7)	(2.5)	(2.2)	(2.4)	(2.2)	(2.0)	
2	7.6	7.4	7.4	5.4	5.3	5.3	4.2	4.2	4.1	4.0	3.9	4.0	3.7	3.6	3.7	
	(5.0)	(5.0)	(5.0)	(3.8)	(3.6)	(4.0)	(3.0)	(3.0)	(3.0)	(2.1)	(2.1)	(2.0)	(2.0)	(2.0)	(2.0)	
2.5	7.1	7.1	7.1	5.0	5.0	5.0	4.0	4.0	4.0	3.6	3.5	3.7	3.2	3.2	3.2	
	(5.0)	(5.0)	(5.0)	(3.1)	(3.1)	(3.0)	(2.9)	(2.9)	(3.0)	(2.0)	(2.0)	(2.0)	(2.0)	(2.0)	(2.0)	
SDRL	EARL	19.5	15.9	12.3	17.9	14.2	10.0	16.9	12.8	8.5	15.8	12.3	9.2	16.0	12.3	8.9
		(8.1)	(7.6)	(6.7)	(6.2)	(5.7)	(5.0)	(5.3)	(4.8)	(4.1)	(4.7)	(4.2)	(3.4)	(4.6)	(4.2)	(3.4)
	0.25	244.1	153.5	213.8	251.2	208.1	179.0	272.2	174.1	132.8	221.1	148.8	265.3	242.7	189.6	302.4
		(4.1)	(3.2)	(1.4)	(4.6)	(3.4)	(1.5)	(4.9)	(3.8)	(1.6)	(5.0)	(3.8)	(1.7)	(5.1)	(4.0)	(1.8)
	0.5	6.8	4.9	2.3	6.7	4.8	2.3	7.4	4.7	2.5	7.9	4.9	2.7	7.6	4.8	2.6
		(1.3)	(1.1)	(0.6)	(1.3)	(1.0)	(0.5)	(1.3)	(1.1)	(0.6)	(1.4)	(1.1)	(0.5)	(1.5)	(1.2)	(0.5)
	0.75	2.1	1.7	1.1	2.1	1.7	1.0	2.3	1.7	1.1	2.4	1.8	1.1	2.5	1.9	1.1
		(0.7)	(0.7)	(0.5)	(0.7)	(0.6)	(0.3)	(0.7)	(0.6)	(0.3)	(0.7)	(0.7)	(0.4)	(0.8)	(0.7)	(0.3)
1	1.3	1.0	0.7	1.2	1.0	0.7	1.2	1.0	0.6	1.3	1.1	0.7	1.3	1.1	0.7	
	(0.6)	(0.5)	(0.1)	(0.5)	(0.5)	(0.2)	(0.5)	(0.5)	(0.3)	(0.5)	(0.5)	(0.3)	(0.5)	(0.5)	(0.3)	
1.5	0.6	0.6	0.6	0.6	0.5	0.4	0.6	0.6	0.5	0.6	0.5	0.3	0.6	0.5	0.4	
	(0.5)	(0.5)	(0.1)	(0.3)	(0.5)	(0.2)	(0.5)	(0.5)	(0.0)	(0.5)	(0.5)	(0.1)	(0.5)	(0.4)	(0.0)	
2	0.5	0.5	0.5	0.5	0.2	0.4	0.4	0.4	0.3	0.3	0.4	0.2	0.5	0.5	0.4	
	(0.1)	(0.1)	(0.0)	(0.2)	(0.4)	(0.1)	(0.5)	(0.4)	(0.0)	(0.3)	(0.3)	(0.0)	(0.0)	(0.0)	(0.0)	
2.5	0.2	0.3	0.2	0.2	0.2	0.1	0.1	0.1	0.1	0.3	0.4	0.2	0.4	0.4	0.3	
	(0.0)	(0.0)	(0.0)	(0.2)	(0.3)	(0.0)	(0.4)	(0.4)	(0.0)	(0.1)	(0.1)	(0.0)	(0.0)	(0.0)	(0.0)	
ESDRL	36.5	23.2	31.3	37.5	30.9	26.3	40.6	26.1	19.7	33.4	22.6	38.6	36.5	28.4	44.0	
	(1.0)	(0.9)	(0.4)	(1.1)	(1.0)	(0.4)	(1.3)	(1.0)	(0.4)	(1.2)	(1.0)	(0.4)	(1.2)	(1.0)	(0.4)	

the process location, the $SRR_{2\text{-of-}(2+v)}$ and $IRR_{2\text{-of-}(2+v)}$ W-HEWMA RSS charts are similar in performance, whereas, for moderate-to-large shifts, the $IRR_{2\text{-of-}(2+v)}$ W-HEWMA RSS chart is more sensitive than the $SRR_{2\text{-of-}(2+v)}$ W-HWMA RSS chart regardless of the nature of the process underlying distribution.

5.6. *Comparison with the Existing W-EWMA and W-DEWMA Charts.* In this section, the performance of the proposed W-HEWMA chart is compared to that of the existing W-EWMA and W-DEWMA charts using SRS and RSS techniques by Li et al. [30], Malela-Majika and Rapoo [47], and Malela-Majika [48]. In Table 4, the performances of the W-HEWMA chart is compared to the W-DEWMA and W-EWMA schemes under the $N(0,1)$, $t(5)$, and $G(1,1)$ distributions when $\eta = 0.05$, $(\eta_1, \eta_2) = (0.05, 0.9)$. Firstly, it is observed that RSS technique's ARL and EARL values are smaller than those of the corresponding SRS technique. Secondly, under the SRS technique, it can be observed that the W-HEWMA chart outperforms the W-DEWMA chart for small-to-large shifts, and it is more sensitive than the W-EWMA chart for small-to-moderate shifts in the process

location; on the other hand, for large shifts, the W-HEWMA and W-EWMA charts are almost similar in ARL performance. Moreover, the W-DEWMA chart outperforms the basic W-EWMA chart for small shifts and the converse is true for moderate-to-large shifts in the process location. Thirdly, under the RSS technique, the W-HEWMA chart outperforms the W-EWMA chart for small shifts, whereas, for moderate-to-large shifts, the two charts are almost equivalent. Moreover, the W-HEWMA chart is superior to the W-DEWMA chart regardless of the size of the shift, and the W-DEWMA chart outperforms the W-EWMA chart except for moderate-to-large shifts. Finally, the SDRL results show that, under symmetric distributions, W-HEWMA SRS chart is preferred over the W-EWMA and W-DEWMA SRS charts for small and large shifts. Under skewed and heavy-tailed distributions, the W-DEWMA SRS chart is more reliable for small shifts than the W-EWMA and W-HEWMA SRS charts, whereas for moderate shifts the W-HEWMA SRS chart is more reliable. However, for large shifts, the three charts are equivalent in terms of the OOC SDRL values. The W-DEWMA and HEWMA RSS charts are both more reliable than the W-EWMA RSS chart in terms of the OOC SDRL profile for small shifts; however, for

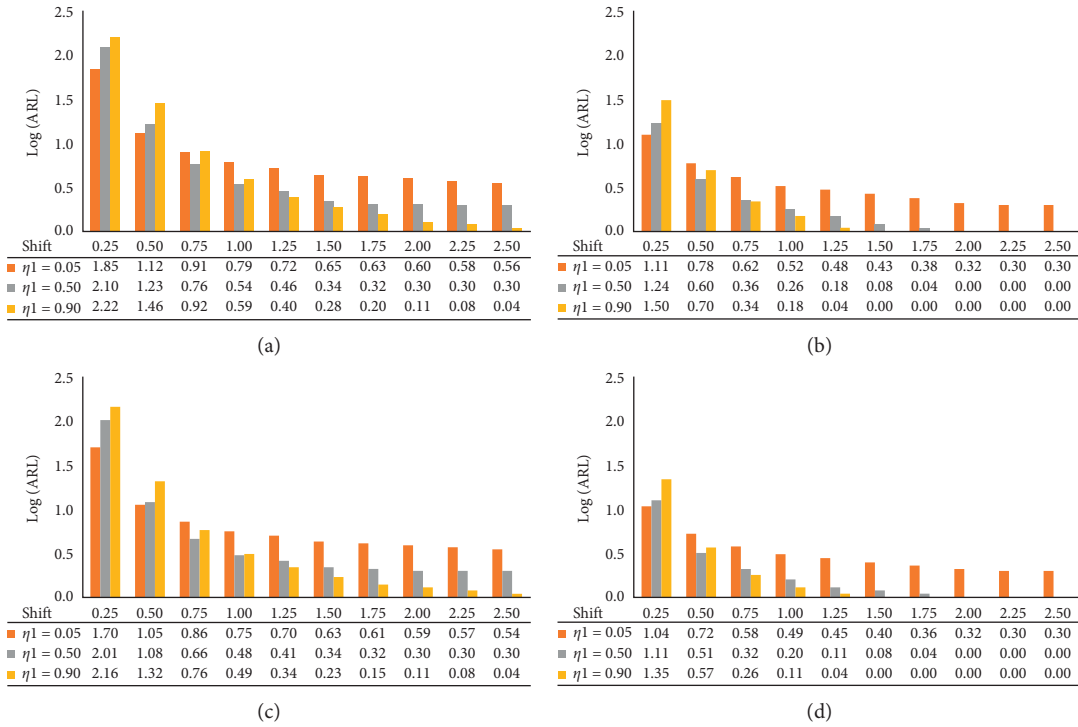


FIGURE 1: OOC $\log(\text{ARL})$ profiles comparisons of the W-HEWMA SRS and RSS charts when $\eta_1 \in \{0.05, 0.50, 0.90\}$, $\eta_2 = 0.75$, $(m, n) = (100, 5)$ for a nominal ARL value of 500. (a) SRS technique under $N(0,1)$ distribution. (b) RSS technique under $N(0,1)$ distribution. (c) SRS technique under $t(5)$ distribution. (d) RSS technique under $t(5)$ distribution.

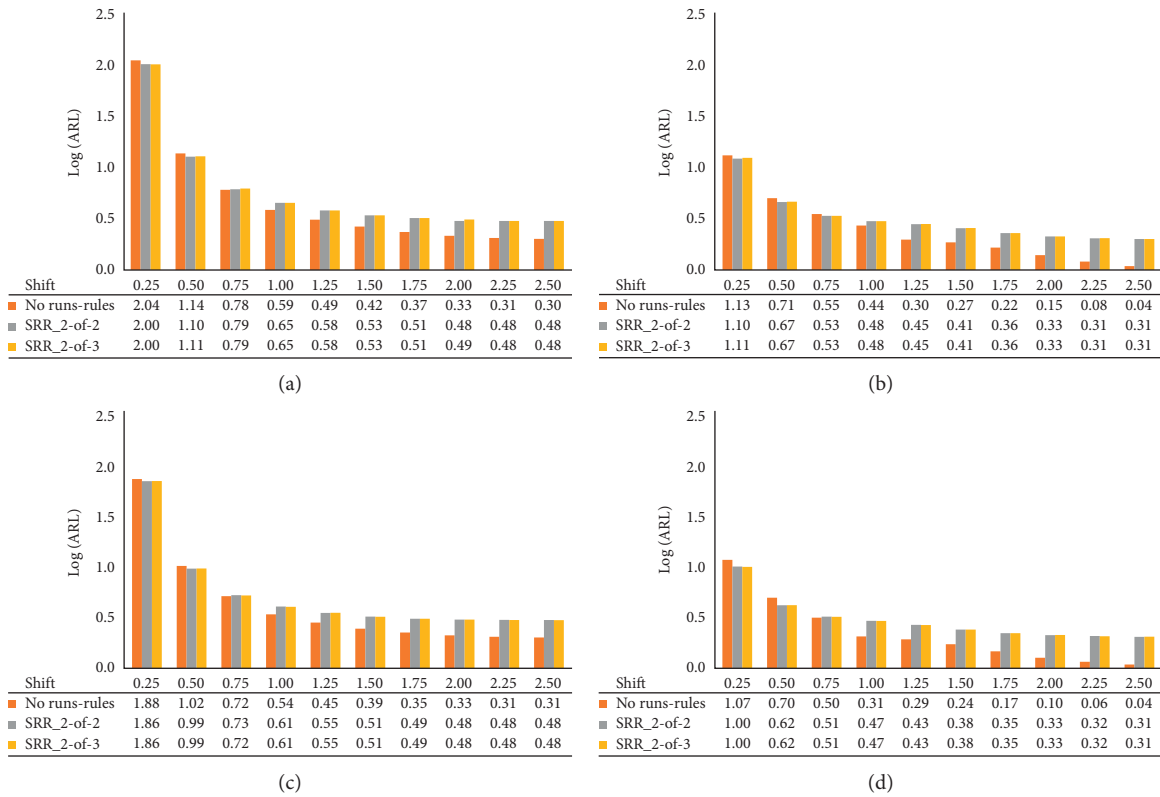


FIGURE 2: OOC $\log(\text{ARL})$ profiles comparisons of the $\text{SRR}_{2\text{-of-}(2+v)}$ W-HEWMA SRS and RSS charts with and without runs-rules when $v \in \{0, 1\}$, $(m, n) = (100, 5)$, $(\eta_1, \eta_2) = (0.25, 0.75)$ for a nominal ARL of 500. (a) SRS technique under $N(0,1)$ distribution. (b) RSS technique under $N(0,1)$ distribution. (c) SRS technique under $t(5)$ distribution. (d) RSS technique under $t(5)$ distribution.

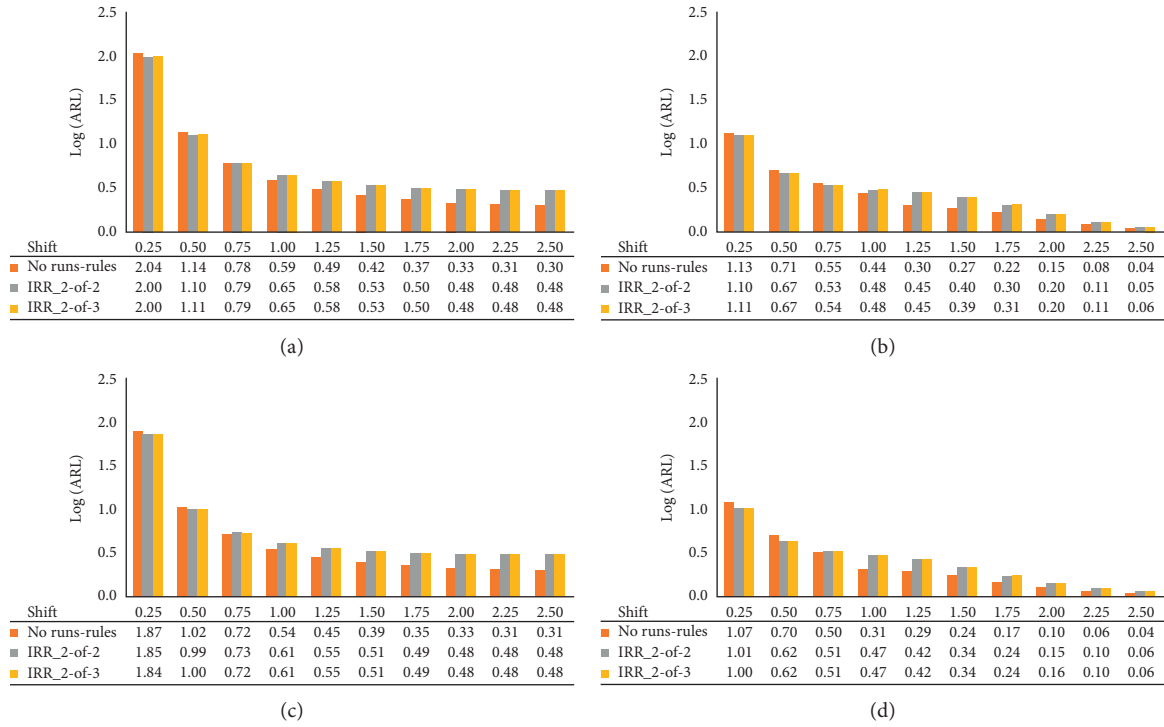


FIGURE 3: OOC log(ARL) profiles comparisons of the $IRR_{2\text{-of-}(2+v)}$ W-HEWMA SRS and RSS charts with and without runs-rules when $v = 0$ and 1 , $(m, n) = (100, 5)$, $(\eta_1, \eta_2) = (0.25, 0.75)$ for a nominal ARL of 500. (a) SRS technique under $N(0,1)$ distribution. (b) RSS technique under $N(0,1)$ distribution. (c) SRS technique under $t(5)$ distribution. (d) RSS technique under $t(5)$ distribution.

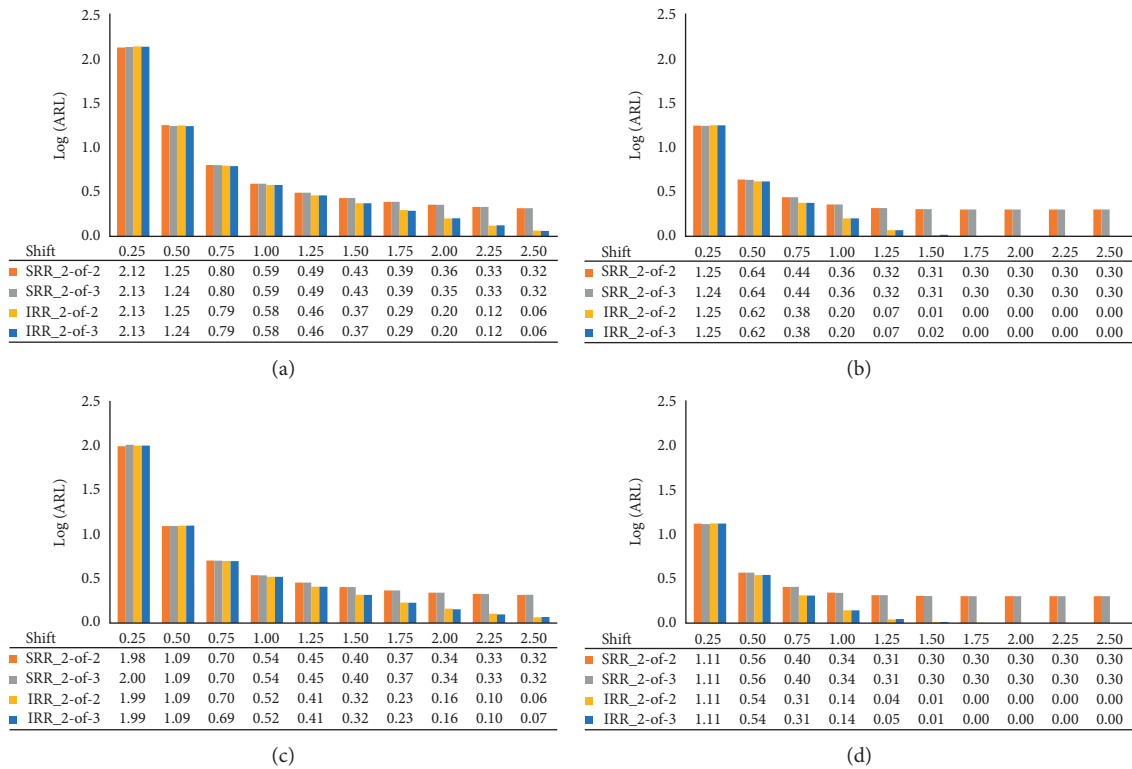


FIGURE 4: OOC ARL profiles comparisons of the $SRR_{2\text{-of-}(2+v)}$ and $IRR_{2\text{-of-}(2+v)}$ W-HEWMA SRS and RSS schemes when $v \in \{0, 1\}$, $(m, n) = (100, 5)$, and $(\eta_1, \eta_2) = (0.5, 0.9)$ for a nominal ARL of 500. (a) SRS technique under $N(0,1)$ distribution. (b) RSS technique under $N(0,1)$ distribution. (c) SRS technique under $t(5)$ distribution. (d) RSS technique under $t(5)$ distribution.

TABLE 4: OOC ARL and SDRL profile comparisons of the basic HEWMA SRS (and RSS in parentheses) charts with the W-EWMA and W-DEWMA SRS and RSS schemes when $(m, n) = (100, 5)$ for a nominal ARL_0 of 500.

Shift	N(0,1)			t(5)			G(1,1)			
	EWMA	DEWMA	HEWMA	EWMA	DEWMA	HEWMA	EWMA	DEWMA	HEWMA	
ARL	0.00	497.4 (498.2)	510.5 (498.8)	496.4 (503.4)	505.7 (499.4)	498.8 (502.3)	498.6 (501.9)	496.4 (497.5)	502.8 (501.8)	500.5 (500.4)
	0.25	79.2 (16.7)	75.8 (16.2)	73.5 (12.9)	55.1 (14.8)	52.6 (14.3)	51.6 (11.0)	36.3 (10.4)	34.0 (9.6)	32.1 (7.4)
	0.50	18.4 (9.8)	16.8 (9.3)	13.3 (5.9)	17.2 (7.6)	14.8 (7.1)	11.1 (5.2)	13.3 (6.7)	12.8 (6.4)	8.3 (4.1)
	0.75	13.6 (4.8)	12.4 (6.7)	8.0 (4.0)	11.2 (4.2)	10.3 (6.4)	7.1 (3.7)	11.7 (3.7)	9.7 (6.3)	5.9 (3.1)
	1.00	7.9 (3.1)	9.1 (6.4)	6.0 (3.2)	7.4 (2.9)	8.3 (6.2)	5.5 (3.0)	6.8 (2.8)	7.5 (6.2)	4.9 (2.9)
	1.50	6.3 (2.3)	7.7 (6.0)	4.3 (2.4)	6.1 (2.1)	7.1 (6.1)	4.1 (2.2)	5.0 (2.0)	6.2 (6.0)	4.0 (2.0)
	2.00	4.6 (2.0)	6.7 (6.0)	3.7 (2.0)	4.5 (2.0)	6.4 (6.0)	3.6 (2.0)	3.8 (2.0)	6.0 (6.0)	3.7 (2.0)
2.50	3.4 (2.0)	6.0 (6.0)	3.2 (2.0)	3.1 (2.0)	6.0 (6.0)	3.2 (2.0)	3.0 (2.0)	6.0 (6.0)	3.2 (2.0)	
SDRL	EARL	191 (5.8)	192 (8.1)	16.0 (4.6)	14.9 (5.1)	15.1 (7.4)	12.3 (4.2)	11.4 (4.2)	11.7 (6.6)	8.9 (3.4)
	0.00	914.0 (488.7)	915.7 (504.6)	880.8 (515.0)	863.3 (513.7)	856.3 (518.3)	871.2 (511.7)	841.1(507.0)	859.7 (506.6)	875.7 (519.0)
	0.25	271.2 (6.1)	243.7 (4.0)	242.7 (5.1)	164.1 (5.1)	106.6 (3.2)	189.6 (4.0)	174.9 (2.7)	172.8 (1.5)	302.4 (1.8)
	0.50	8.2 (2.1)	6.9 (1.3)	7.6 (1.5)	5.9 (1.9)	5.2 (1.2)	4.8 (1.2)	2.6 (1.1)	2.5 (0.6)	2.6 (0.5)
	0.75	3.4 (1.0)	3.3 (0.8)	2.5 (0.8)	1.9 (1.0)	1.8 (0.7)	1.9 (0.7)	2.6 (0.5)	2.5 (0.4)	2.6 (0.3)
	1.00	1.4 (0.5)	2.4 (0.6)	1.3 (0.5)	1.1 (0.5)	1.2 (0.5)	1.1 (0.5)	1.1 (0.4)	1.0 (0.3)	0.7 (0.3)
	1.50	0.6 (0.1)	0.7 (0.3)	0.6 (0.5)	0.6 (0.3)	0.6 (0.4)	0.5 (0.4)	0.6 (0.0)	0.5 (0.0)	0.4 (0.0)
2.00	0.5 (0.1)	0.5 (0.0)	0.5 (0.0)	0.5 (0.1)	0.5 (0.0)	0.5 (0.0)	0.5 (0.0)	0.5 (0.0)	0.4 (0.0)	
2.50	0.3 (0.0)	0.2 (0.0)	0.4 (0.0)	0.3 (0.0)	0.3 (0.0)	0.4 (0.0)	0.3 (0.0)	0.2 (0.0)	0.3 (0.0)	
ESDRL	40.8 (1.4)	36.8 (1.0)	36.5 (1.2)	24.9 (1.3)	16.6 (0.9)	28.4 (1.0)	26.1 (0.7)	25.7 (0.4)	44.2 (0.4)	

TABLE 6: Phase I sample of the iron ore data.

Sample number	1	2	3	4	5
1	3.05	1.13	1.17	1.33	1.21
2	2.10	1.79	1.08	1.81	1.65
3	1.01	1.33	1.64	1.85	1.58
4	1.09	1.88	2.20	1.48	1.42
5	2.15	1.22	1.63	1.38	1.80
6	1.91	1.90	1.28	1.24	2.43
7	1.25	1.84	1.26	1.37	1.19
8	1.44	1.06	1.60	1.16	1.09
9	2.72	1.52	1.44	4.15	4.95
10	1.32	1.85	2.05	2.59	1.50
11	2.29	1.74	1.43	1.71	1.62
12	3.96	1.63	1.57	2.05	1.39
13	3.36	1.01	2.06	3.36	3.36
14	0.97	3.80	3.36	1.73	3.36
15	1.69	2.56	1.47	1.90	1.90
16	1.63	1.61	1.79	2.05	2.93
17	2.04	1.30	1.44	1.32	1.59
18	1.49	2.05	2.36	2.34	1.33
19	2.10	1.48	1.51	2.77	3.42
20	1.67	1.48	1.48	1.88	2.16
21	2.10	1.74	1.79	2.44	1.88
22	1.81	1.67	2.10	1.78	2.54
23	1.58	1.57	1.45	1.92	2.20
24	1.62	1.71	2.65	1.72	2.44
25	5.21	1.10	1.61	2.72	1.94
26	3.01	1.61	1.45	1.69	1.62
27	1.70	1.89	2.28	2.45	2.14
28	1.72	1.66	1.92	2.71	1.73
29	1.83	1.47	1.35	1.58	1.74
30	1.24	1.47	1.10	1.87	1.62
31	1.76	1.94	1.46	1.39	1.91
32	1.87	1.98	2.32	2.22	1.57
33	1.68	2.08	1.78	1.18	2.32
34	2.30	1.56	2.32	1.48	1.13
35	1.39	3.63	2.80	1.69	4.32
36	2.01	3.56	1.65	1.48	2.10
37	2.23	1.64	2.67	1.92	3.14
38	2.81	2.01	2.22	2.64	3.84
39	2.40	2.40	2.40	1.37	2.40
40	1.59	1.44	2.40	1.78	2.40
41	2.68	1.60	1.04	2.40	1.56
42	1.10	1.10	1.02	2.40	1.10
43	1.20	1.00	1.09	3.70	3.17
44	1.69	1.86	1.44	1.49	2.19
45	1.05	3.21	1.62	1.22	1.10
46	0.96	1.81	1.33	0.86	3.27
47	3.27	1.09	4.15	3.81	1.40
48	1.86	1.22	1.99	1.45	4.09
49	4.83	2.17	1.64	1.63	1.69
50	1.63	1.42	1.95	1.94	2.61
51	1.93	1.53	4.92	1.93	1.22
52	2.21	2.21	2.26	1.33	1.93
53	1.24	2.04	3.21	1.76	1.41
54	1.67	1.74	1.93	2.41	1.46
55	1.75	1.27	1.13	1.78	3.06
56	2.40	1.80	2.31	2.56	1.50
57	1.26	3.17	4.73	2.28	1.14
58	1.79	1.28	1.52	1.17	1.14
59	1.76	2.42	1.28	2.12	1.11
60	1.19	1.01	1.28	3.14	1.55

TABLE 6: Continued.

Sample number	1	2	3	4	5
61	2.24	1.27	2.10	2.20	1.10
62	1.59	2.20	1.37	1.64	2.11
63	1.34	1.76	1.53	1.30	1.34
64	4.12	1.34	1.34	1.34	1.34
65	2.62	1.87	1.16	1.51	1.12
66	1.91	1.34	1.86	1.34	1.91
67	1.28	1.38	1.04	3.17	1.49
68	1.08	1.16	1.32	2.13	3.87
69	1.18	1.05	1.05	1.73	1.29
70	1.42	1.60	1.52	1.33	1.30
71	1.42	1.23	1.25	1.28	1.11
72	1.36	1.47	1.04	1.27	1.88
73	3.17	3.02	3.55	3.48	1.82
74	1.41	1.24	1.05	1.08	2.32
75	0.94	1.29	1.40	1.81	1.00
76	1.08	1.66	1.06	1.59	1.62
77	1.62	2.08	1.44	1.41	2.24
78	1.53	1.27	2.26	1.62	1.13
79	4.73	1.70	3.22	4.12	1.80
80	1.62	5.45	1.62	2.49	1.63
81	2.83	2.55	1.37	1.08	1.58
82	1.90	1.82	1.88	1.49	1.46
83	1.61	4.65	0.99	1.36	1.35
84	2.49	1.33	1.40	1.30	1.21
85	1.49	1.32	1.27	1.32	1.54
86	1.73	1.32	1.59	1.83	1.41
87	1.73	1.37	1.98	4.32	1.50
88	1.84	1.51	1.36	4.55	1.72
89	1.25	3.25	1.92	1.33	2.26
90	4.04	1.93	1.38	1.57	1.43
91	1.32	1.32	3.03	1.32	3.03
92	3.68	1.32	2.06	1.32	1.32
93	1.51	1.23	1.91	2.41	2.15
94	2.11	3.25	2.24	2.55	1.26
95	1.93	2.87	1.59	2.83	2.02
96	2.14	1.49	1.68	2.30	2.11
97	1.65	1.92	1.33	3.87	1.09
98	1.69	1.24	1.78	1.60	1.62
99	2.16	1.68	1.68	1.58	2.92
100	1.21	1.56	3.72	2.17	1.68
101	2.05	2.19	2.03	2.01	2.20
102	4.64	2.21	1.54	2.19	1.66
103	1.02	1.68	1.53	1.04	1.79
104	3.12	2.03	0.97	1.99	1.42
105	2.63	2.07	2.09	1.23	1.85
106	1.37	2.50	1.26	1.08	1.37
107	3.30	2.20	1.34	1.34	4.57
108	2.41	2.11	1.34	3.49	1.61
109	2.97	1.79	1.90	1.73	1.61
110	2.99	2.67	1.56	1.52	2.92

moderate-to-large shifts, the three competing charts are almost equivalent.

Next, using $\eta = 0.5$ and $(\eta_1, \eta_2) = (0.5, 0.9)$ in Table 5, under SRS technique, it is observed that in general the IRR_{2-of-3} W-DEWMA chart outperforms the other competitors (see the EARL values), with the IRR_{2-of-3} W-HEWMA chart in the second place. However, under RSS technique, the IRR_{2-of-3} W-HEWMA chart outperforms the other charts in terms of the EARL.

6. Illustrative Example

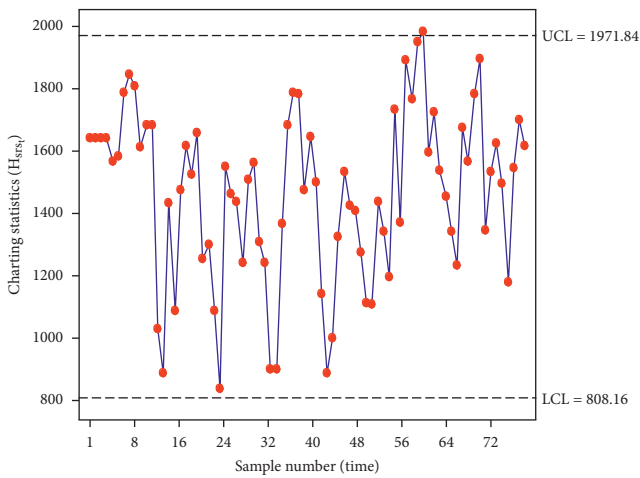
In this section, the proposed W-HEWMA SRS and RSS schemes are implemented using mining real-life data to monitor the silicon dioxide percentage in iron ore in order to refine flotation process from Mukherjee et al. [32]. Silica high concentration in the final ore is a sign of impurity and is therefore not desired. Thus, it is very important to continuously monitor the flotation process of silica concentrate

TABLE 7: Phase II iron ore data.

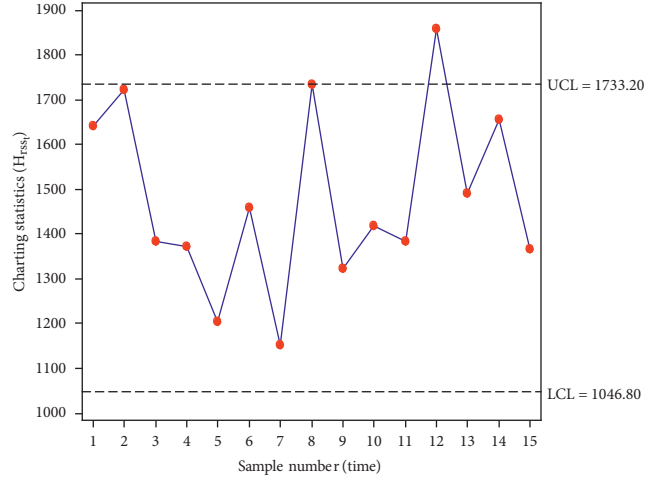
Sample number	1	2	3	4	5
1	2.08	2.08	2.08	2.08	2.08
2	2.08	2.08	2.08	2.08	2.08
3	2.08	2.08	2.08	2.08	2.08
4	2.08	2.08	2.08	2.08	2.08
5	2.08	2.08	1.59	2.08	2.08
6	1.65	2.08	2.08	2.08	2.08
7	4.32	1.67	2.05	5.42	3.84
8	1.75	5.42	5.35	4.33	4.33
9	2.1	3.64	3.88	3.07	2
10	2	1.24	3.64	3.13	3.13
11	1.79	1.97	2.36	2.41	2.47
12	4.52	2.44	1.69	1.73	1.73
13	1.13	1.55	1.25	1.08	1.58
14	1.04	1.42	1.09	1.16	1.16
15	1.02	1.34	1.92	4.7	2.39
16	1.21	0.91	1.27	1.32	1.32
17	1.49	2.32	2.06	1.39	2.17
18	3.36	2.16	4.65	1.56	1.56
19	1.56	1.66	1.56	3.8	2.62
20	5.52	1.47	4.14	1.57	1.57
21	1.22	1.84	1.29	1.68	1.82
22	1.15	1.66	1.97	2.29	2.29
23	1.92	1.33	1.25	1.2	1.31
24	0.74	0.6	1.29	1.11	1.11
25	2.49	2.59	1.17	2.64	1.70
26	2.72	2.65	1.3	1.88	1.88
27	1.39	1.57	2.61	1.48	2.64
28	1.86	1.35	1.25	1.28	1.28
29	1.66	1.8	2.21	1.59	2.21
30	1.72	1.96	2.21	1.68	1.68
31	2.06	1.17	1.35	1.57	2.19
32	1.37	2.1	1.51	1.49	1.49
33	1.19	1.19	1.19	1.19	1.19
34	1.19	1.19	1.19	1.19	1.19
35	4.86	1.19	1.67	1.19	2.12
36	1.66	2.47	3.69	1.61	1.61
37	2.92	2.51	5.53	2.25	1.88
38	2.13	4.33	2.02	3.58	3.58
39	1.58	1.51	2.16	2.17	1.87
40	4.14	3.66	1.26	3.18	3.18
41	1.89	1.35	1.24	4.35	4.57
42	1.78	1.2	1.29	1	1
43	1.11	1.42	1.14	0.94	1.02
44	1.37	1.54	1.19	1.26	1.26
45	2.46	1.39	1.23	2.33	1.33
46	2.92	2.46	1.73	1.41	1.41
47	1.31	2.93	2	2.2	1.27
48	1.7	2.12	1.79	1.44	1.44
49	0.84	1.45	2.12	3	1.21
50	1.18	2.3	0.87	1.56	1.56
51	1.52	1.49	1.29	1.51	1.24
52	1.28	1.81	1.39	3.39	3.39
53	1.52	2.24	1.84	1.3	1.59
54	1.44	1.14	1.42	1.75	1.75
55	3.53	1.81	2.85	5.53	1.67
56	4.71	1.35	1.13	2.85	2.85
57	4.06	2.04	3.77	4.07	3.95
58	2.82	3.66	1.63	2.58	2.58
59	4.61	4.14	2.72	5.08	3.50
60	4.99	4.62	4.04	4.79	4.79

TABLE 7: Continued.

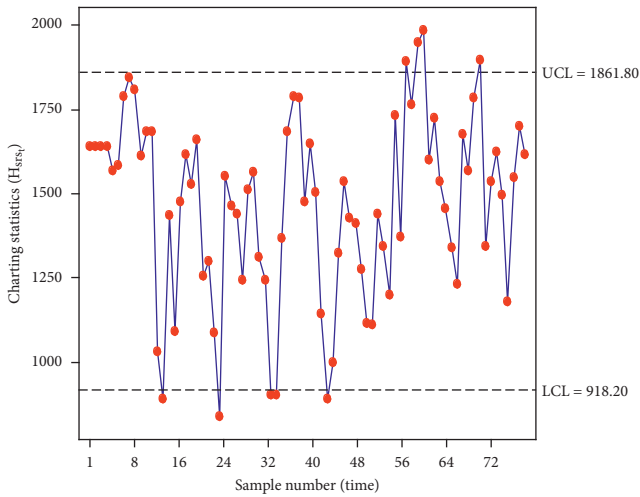
Sample number	1	2	3	4	5
61	2.49	1.63	1.53	4.12	2.09
62	2.77	4.07	1.97	1.76	1.76
63	3.2	2.55	1.96	1.4	1.58
64	1.41	1.6	1.41	3.18	3.18
65	3.98	1.33	1.24	4.44	1.00
66	1.31	5.29	1.15	1.65	1.65
67	3.71	2.7	1.66	3.95	1.57
68	1.22	1.76	3.16	2.31	2.31
69	2.47	2.3	2.41	2.25	2.83
70	2.71	4.89	4.08	4.87	4.87
71	1.78	1.49	2.48	1.29	1.60
72	2.74	1.73	1.82	3.31	3.31
73	2.57	3.01	2.41	1.76	1.49
74	2.47	2.46	1.21	2.23	2.23
75	1.42	1.25	1.5	1.65	1.57
76	1.79	1.99	2.4	1.77	1.77
77	2.36	1.83	1.93	2.87	2.46
78	1.71	1.7	3.07	1.71	1.71



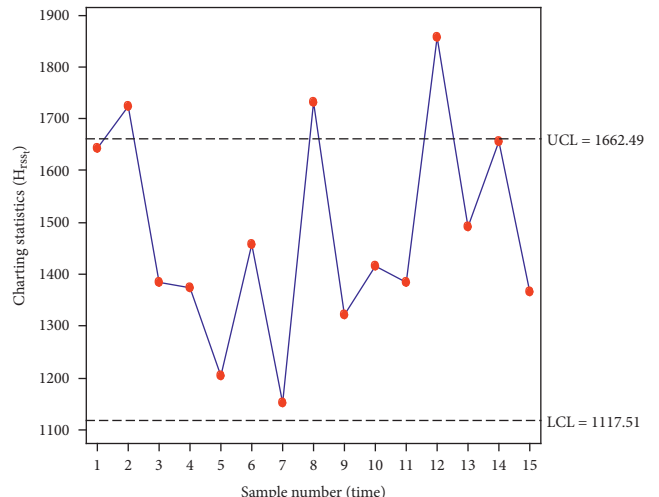
(a)



(b)



(c)



(d)

FIGURE 5: Continued.

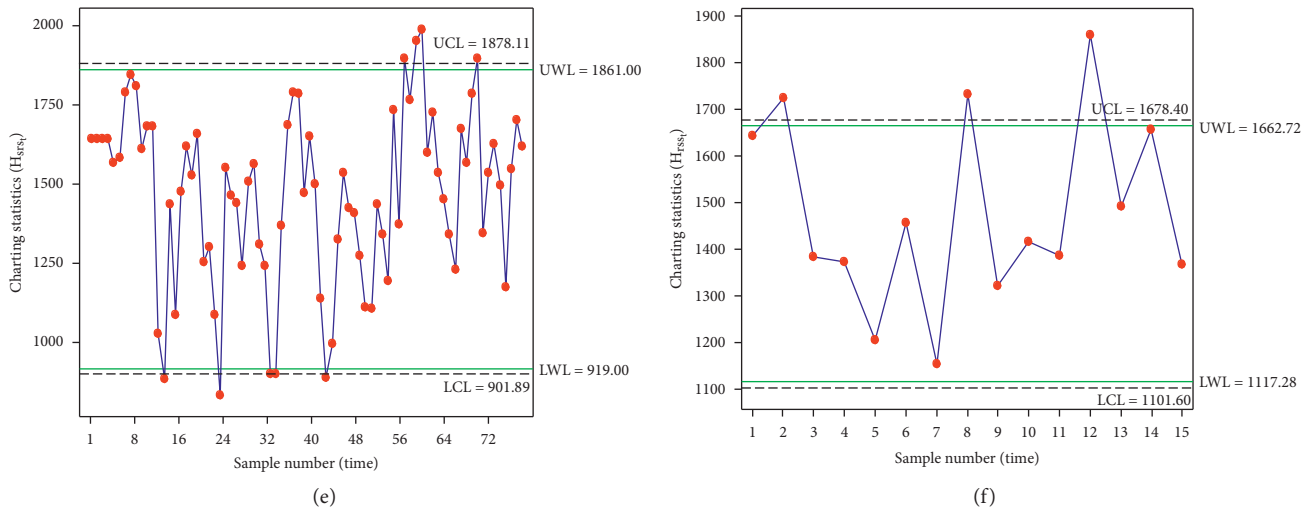


FIGURE 5: Illustration examples of the proposed W-HEWMA SRS and RSS charts with and without runs-rules using the iron ores data. (a) W-HEWMA SRS chart. (b) W-HEWMA RSS chart. (c) SRR_{2-of-3} W-HEWMA SRS chart. (d) SRR_{2-of-3} W-HEWMA RSS chart. (e) IRR_{2-of-3} W-HEWMA SRS chart. (f) IRR_{2-of-3} W-HEWMA RSS chart.

in iron ore in order to fix any abnormality or problem that may arise. Therefore, in this paper, the W-HEWMA scheme with and without runs-rules is used for this purpose.

The mining data contains two sets of data considered as Phases I and II data, shown in Tables 6 and 7, respectively. However, in addition to the data from Mukherjee et al. [32], in this paper, we assume that every half an hour a subgroup of size five is taken. Thus, in Phase I, 110 samples of size 5 (i.e., $m = 550$) are collected when the process is deemed IC. In Phase II, there are 78 subgroups of size 5 (i.e., $n = 5$) each. In case of the RSS, at each sampling time t , the judgement ranking begins by collecting (or considering) 5 samples of size $n = 5$, ordering them according to the operator judgement from the smallest to the largest, and lastly selecting the n diagonal elements. In this example, it is assumed that there is a perfect judgement ranking. The W-HEWMA schemes are implemented when $(\eta_1, \eta_2) = (0.5, 0.9)$ with a nominal ARL_0 of 500. The control limit constants of the basic, SRR_{2-of-3} , and IRR_{2-of-3} W-HEWMA SRS schemes are found to be equal to 2.9689, 2.4074, and (2.4906, 2.4033) so that they yield the attained ARL_0 values of 502.7, 501.9, and 500.8, respectively. However, the control limit constants of the basic, SRR_{2-of-3} , and IRR_{2-of-3} W-HEWMA RSS schemes are found to be equal to 1.7512, 1.3904, and (1.4716, 1.3916) so that they yield the attained ARL_0 values of 500.6, 501.7, and 502.0, respectively. The plots of the proposed W-HEWMA schemes are shown in Figure 5. From this figure, it can be seen that, on the one hand, the basic W-HEWMA SRS scheme gives a signal for the first on the 60th subgroup (see Figure 5(a)), whereas both the SRR_{2-of-3} and IRR_{2-of-3} W-HEWMA SRS schemes give a signal on the 14th subgroup in the prospective phase (i.e., Phase II); see Figures 5(c) and 5(e). On the other hand, the basic W-HEWMA RSS scheme gives a signal for the first on the 12th subgroup (see Figure 5(b)), whereas both the SRR_{2-of-3} and IRR_{2-of-3} W-HEWMA RSS schemes give a signal on the 2nd subgroup; see Figures 5(d) and 5(f).

Therefore, this real-life illustrative example shows that the SRR_{2-of-3} and IRR_{2-of-3} W-HEWMA schemes are more sensitive than the basic W-HEWMA schemes in this particular case.

7. Concluding Remarks

New distribution-free HEWMA monitoring schemes based on the W statistic using SRS and RSS sampling designs based on perfect judgement ranking are proposed. The proposed W-HEWMA SRS and RSS schemes are further improved using supplementary standard and improved runs-rules. The abilities of the new distribution-free HEWMA monitoring schemes are evaluated in terms of the ARL and SDRL profiles. The characteristics of the proposed schemes revealed that they perform better under skewed and heavy-tailed distributions. It is also found that the choice of the magnitude of the smoothing parameters depends on the shift of interest. For instance, when the detection of large shifts is of interest, it is recommended that two large smoothing parameters are combined. However, when the detection of small shifts is of interest, it is recommended that small smoothing parameters are combined. In case the detection of moderate shifts is of interest, the combination of moderate values of the smoothing parameters is recommended. Small-to-large shifts will be detected quickly when combining small and large smoothing parameters. From the results obtained in this study, in terms of the performance ability of the proposed schemes, operators are recommended to use the proposed $IRR_{2-of-(2+v)}$ W-HEWMA scheme based on SRS or RSS technique when small-to-large shifts are of interest. Moreover, the basic W-HEWMA schemes are most preferred over the basic W-EWMA and W-DEWMA schemes.

Since this research is based on perfect judgement ranking, the corresponding research on imperfect judgement ranking is already under way. For future research

purpose, interested researchers can also investigate the performance of the composite Shewhart-HEWMA scheme based on the W statistic using the SRS and RSS schemes. The synthetic W -HEWMA scheme using SRS and RSS techniques can also be investigated. Finally, only the basic RSS design is considered here; hence, other modifications of the RSS can also be studied in the future, i.e., extreme, median, neuteric, ordered perfect, and imperfect RSS (see, for instance, [38, 56]).

Data Availability

The raw data used to illustrate the implementation of the proposed control chart is given in Tables 6 and 7, and its characteristics are explained in Section 6.

Conflicts of Interest

The authors declare that they have no conflicts of interest.

References

- [1] D. C. Montgomery, *Statistical Quality Control: A Modern Introduction*, John Wiley & Sons, Singapore, 7th edition, 2013.
- [2] P. Qiu, *Introduction to Statistical Process Control*, Chapman & Hall/CRC Press, Taylor & Francis Group, Baton Rouge, FL, USA, 2014.
- [3] S. Chakraborti and M. A. Graham, *Nonparametric Statistical Process Control*, Wiley, New York, NY, USA, 2019.
- [4] A. Haq, "A new hybrid exponentially weighted moving average control chart for monitoring process mean," *Quality and Reliability Engineering International*, vol. 29, no. 7, pp. 1015–1025, 2013.
- [5] A. Haq, "A new nonparametric synthetic EWMA control chart for monitoring process mean," *Communications in Statistics - Simulation and Computation*, vol. 48, no. 6, pp. 1665–1676, 2019.
- [6] M. B. C. Khoo, P. Castagliola, J. Y. Liew, W. L. Teoh, and P. E. Maravelakis, "A study on EWMA charts with runs rules—the Markov chain approach," *Communications in Statistics-Theory and Methods*, vol. 45, no. 14, pp. 4156–4180, 2016.
- [7] O. A. Adeoti, "On control chart for monitoring exponentially distributed quality characteristic," *Transactions of the Institute of Measurement and Control*, vol. 42, no. 2, pp. 295–305, 2020.
- [8] V. Alevizakos, K. Chatterjee, and C. Koukouvinos, "Modified EWMA and DEWMA control charts for process monitoring," *Communications in Statistics-Theory and Methods*, pp. 1–25, 2021.
- [9] V. Alevizakos, K. Chatterjee, and C. Koukouvinos, "The extended homogeneously weighted moving average control chart," *Quality and Reliability Engineering International*, vol. 37, no. 5, pp. 2134–2155, 2021.
- [10] A. Bakdi and A. Kouadri, "An improved plant-wide fault detection scheme based on PCA and adaptive threshold for reliable process monitoring: application on the new revised model of Tennessee Eastman process," *Journal of Chemometrics*, vol. 32, no. 5, Article ID e2978, 2018.
- [11] A. Bakdi, W. Bounoua, S. Mekhilef, and L. M. Halabi, "Nonparametric Kullback-divergence-PCA for intelligent mismatch detection and power quality monitoring in grid-connected rooftop PV," *Energy*, vol. 189, Article ID 116366, 2019.
- [12] W. Bounoua, A. B. Benkara, A. Kouadri, and A. Bakdi, "Online monitoring scheme using principal component analysis through Kullback-Leibler divergence analysis technique for fault detection," *Transactions of the Institute of Measurement and Control*, vol. 42, no. 6, pp. 1225–1238, 2020.
- [13] S. E. Shamma and A. K. Shamma, "Development and evaluation of control charts using double exponentially weighted moving averages," *International Journal of Quality, Reliability and Management*, vol. 9, no. 6, pp. 18–26, 1992.
- [14] L. Zhang and G. Chen, "An extended EWMA mean chart," *Quality Technology & Quantitative Management*, vol. 2, no. 1, pp. 39–52, 2005.
- [15] F. Asif, S. Khan, and M. Noor-ul-Amin, "Hybrid exponentially weighted moving average control chart with measurement error," *Iranian Journal of Science and Technology, Transactions A: Science*, vol. 44, no. 3, pp. 801–811, 2020.
- [16] S. Ahmad and I. Musliyar, "A note on "designing of a hybrid exponentially weighted moving average"" *The International Journal of Advanced Manufacturing Technology*, vol. 97, no. 1–4, pp. 375–377, 2018.
- [17] M. Aslam, S. R. Gadde, M. S. Aldosari, and C.-H. Jun, "A hybrid EWMA chart using coefficient of variation," *International Journal of Quality & Reliability Management*, vol. 36, no. 4, pp. 587–600, 2019.
- [18] O. A. Adeoti and S. O. Koleoso, "A hybrid homogeneously weighted moving average control chart for process monitoring," *Quality and Reliability Engineering International*, vol. 36, no. 6, pp. 2170–2186, 2020.
- [19] J. C. Malela-Majika, S. C. Shongwe, and O. A. Adeoti, "A hybrid homogeneously weighted moving average control chart for process monitoring: discussion," *Quality and Reliability Engineering International*, vol. 36, no. 6, pp. 2170–2186, 2021.
- [20] M. Klein, "Two alternatives to the Shewhart \bar{X} Control chart," *Journal of Quality Technology*, vol. 32, no. 4, pp. 427–431, 2000.
- [21] M. B. C. Khoo and K. N. B. Ariffin, "Two improved runs rules for the Shewhart \bar{X} Control chart," *Quality Engineering*, vol. 18, no. 2, pp. 173–178, 2006.
- [22] D. L. Antzoulakos and A. C. Rakitzis, "The revised m-of-k runs rule," *Quality Engineering*, vol. 20, no. 1, pp. 75–81, 2007.
- [23] S. C. Shongwe, "On the design of nonparametric runs-rules schemes using the Markov chain approach," *Quality and Reliability Engineering International*, vol. 36, no. 5, pp. 1604–1621, 2020.
- [24] O. A. Adeoti and J.-C. Malela-Majika, "Double exponentially weighted moving average control chart with supplementary runs-rules," *Quality Technology & Quantitative Management*, vol. 17, no. 2, pp. 142–172, 2020.
- [25] S. H. Sheu and T. C. Lin, "The generally weighted moving average control chart for detecting small shifts in the process mean," *Quality Engineering*, vol. 16, no. 2, pp. 209–231, 2003.
- [26] M. Riaz, N. Abbas, and R. J. M. M. Does, "Improving the performance of CUSUM charts," *Quality and Reliability Engineering International*, vol. 27, no. 4, pp. 415–424, 2011.
- [27] N. Abbas, M. Riaz, and R. J. M. M. Does, "Enhancing the performance of EWMA charts," *Quality and Reliability Engineering International*, vol. 27, no. 6, pp. 821–833, 2011.
- [28] P. E. Maravelakis, P. Castagliola, and M. B. C. Khoo, "Run length properties of run rules EWMA chart using integral equations," *Quality Technology & Quantitative Management*, vol. 16, no. 2, pp. 129–139, 2017.
- [29] F. Wilcoxon, "Individual comparisons by ranking methods," *Biometrics Bulletin*, vol. 1, no. 6, pp. 80–83, 1945.

- [30] S.-Y. Li, L.-C. Tang, and S.-H. Ng, "Nonparametric CUSUM and EWMA control charts for detecting mean shifts," *Journal of Quality Technology*, vol. 42, no. 2, pp. 209–226, 2010.
- [31] J.-C. Malela-Majika and E. Rapoo, "Distribution-free mixed cumulative sum-exponentially weighted moving average control charts for detecting mean shifts," *Quality and Reliability Engineering International*, vol. 33, no. 8, pp. 1983–2002, 2017.
- [32] A. Mukherjee, Z. L. Chong, and M. B. C. Khoo, "Comparisons of some distribution-free CUSUM and EWMA schemes and their applications in monitoring impurity in mining process flotation," *Computers & Industrial Engineering*, vol. 137, Article ID 106059, 2019.
- [33] Z. L. Chong, A. Mukherjee, and M. B. C. Khoo, "Some simplified Shewhart-type distribution-free joint monitoring schemes and its application in monitoring drinking water turbidity," *Quality Engineering*, vol. 32, no. 1, pp. 91–110, 2020.
- [34] K. Mabude, J.-C. Malela-Majika, and S. C. Shongwe, "A new distribution-free generally weighted moving average monitoring scheme for detecting unknown shifts in the process location," *International Journal of Industrial Engineering Computations*, vol. 11, no. 2, pp. 235–254, 2020.
- [35] V. Tercero-Gomez, V. Aguilar-Lleyda, A. Cordero-Franco, and W. Conover, "A distribution-free CUSUM chart for joint monitoring of location and scale based on the combination of Wilcoxon and Mood statistics," *Quality and Reliability Engineering International*, vol. 36, no. 4, pp. 1422–1453, 2020.
- [36] I. S. Triantafyllou, "Wilcoxon-type rank-sum control charts based on progressively censored reference data," *Communications in Statistics-Theory and Methods*, vol. 50, no. 2, pp. 311–328, 2021.
- [37] T. I. Letshedi, J.-C. Malela-Majika, P. Castagliola, and S. C. Shongwe, "Distribution-free triple EWMA control chart for monitoring the process location using the Wilcoxon rank-sum statistic with fast initial response feature," *Quality and Reliability Engineering International*, vol. 37, no. 5, pp. 1996–2013, 2021.
- [38] A. Haq, J. Brown, E. Moltchanova, and A. I. Al-Omari, "Effect of measurement error on exponentially weighted moving average control charts under ranked set sampling schemes," *Journal of Statistical Computation and Simulation*, vol. 85, no. 6, pp. 1224–1246, 2015.
- [39] M. Awais and A. Haq, "An EWMA chart for monitoring process mean," *Journal of Statistical Computation and Simulation*, vol. 88, no. 5, pp. 1003–1025, 2018.
- [40] M. Noor-ul-Amin and M. Tayyab, "Enhancing the performance of exponential weighted moving average control chart using paired double ranked set sampling," *Journal of Statistical Computation and Simulation*, vol. 90, no. 6, pp. 1118–1130, 2020.
- [41] A. Singh and G. K. Vishwakarma, "Improved predictive estimation for mean using the Searls technique under ranked set sampling," *Communications in Statistics-Theory and Methods*, vol. 50, no. 9, pp. 2015–2038, 2019.
- [42] J. T. Terpstra and L. A. Liudahl, "Concomitant-based rank set sampling proportion estimates," *Statistics in Medicine*, vol. 23, no. 13, pp. 2061–2070, 2004.
- [43] H. Chen, E. A. Stasny, and D. A. Wolfe, "Ranked set sampling for efficient estimation of a population proportion," *Statistics in Medicine*, vol. 24, no. 21, pp. 3319–3329, 2005.
- [44] M. Mahdizadeh and E. Strzalkowska-Kominiak, "Resampling based inference for a distribution function using censored ranked set samples," *Computational Statistics*, vol. 32, no. 4, pp. 1285–1308, 2017.
- [45] M. Mahdizadeh, "On entropy-based test of exponentiality in ranked set sampling," *Communications in Statistics-Simulation and Computation*, vol. 44, no. 4, pp. 979–995, 2015.
- [46] M. Mahdizadeh, "On estimating a stress-strength type reliability," *Hacettepe Journal of Mathematics and Statistics*, vol. 47, pp. 243–253, 2018.
- [47] J.-C. Malela-Majika and E. M. Rapoo, "Distribution-free CUSUM and EWMA control charts based on the Wilcoxon rank-sum statistic using ranked set sampling for monitoring mean shifts," *Journal of Statistical Computation and Simulation*, vol. 86, no. 16, pp. 3715–3734, 2016.
- [48] J.-C. Malela-Majika, "New distribution-free memory-type control charts based on the Wilcoxon rank-sum statistic," *Quality Technology & Quantitative Management*, vol. 18, no. 2, pp. 135–155, 2021.
- [49] S. Ganeslingam and S. Ganesh, "Ranked set sampling versus simple random sampling in the estimation of the mean and the ratio," *Journal of Statistics and Management Systems*, vol. 9, no. 2, pp. 459–472, 2006.
- [50] L. L. Bohn and D. A. Wolfe, "Nonparametric two-sample procedures for ranked-set samples data," *Journal of the American Statistical Association*, vol. 87, no. 418, pp. 552–561, 1992.
- [51] S. L. Stokes and T. W. Sager, "Characterization of a ranked-set sample with application to estimating distribution functions," *Journal of the American Statistical Association*, vol. 83, no. 402, pp. 374–381, 1988.
- [52] D. A. Wolfe, "Ranked set sampling: an approach to more efficient data collection," *Statistical Sciences*, vol. 19, no. 4, pp. 636–643, 2004.
- [53] A. Amro and M. Samoh, *Ranked Set Sampling (RSS): The Second Students Innovation Conference, Hebron, State of Palestine*, Palestine Polytechnic University, Hebron, Palestinian, 2013.
- [54] S. S. Alkahtani, "Robustness of DEWMA versus EWMA control charts to non-normal processes," *Journal of Modern Applied Statistical Methods*, vol. 12, no. 1, pp. 148–163, 2013.
- [55] S. C. Shongwe, J.-C. Malela-Majika, and P. Castagliola, "A combined mixed-s-skip sampling strategy to reduce the effect of autocorrelation on the \bar{X} scheme with and without measurement errors," *Journal of Applied Statistics*, vol. 48, no. 7, pp. 1243–1268, 2020.
- [56] T. Nawaz and D. Han, "Monitoring the process location by using new ranked set sampling-based memory control charts," *Quality Technology & Quantitative Management*, vol. 17, no. 3, pp. 255–284, 2020.